Detection Performance of Spatial-Frequency Diversity MIMO Radar

HONGWEI LIU, Member, IEEE
SHENGHUA ZHOU
HONGTAO SU
Xidian University,
Xi'an, China

YAO YU
Rutgers, The State University of New Jersey,
Piscataway, NJ, USA

For spatial-frequency diversity radar, diversity channels may receive partially correlated target returns and channel signal-to-noise ratios (SNRs) may be different. For six typical scenarios of diversity radar, we design detection algorithms and analyze their detection performances in theory and via numerical results. It is shown that the detectors considering target correlation and channel SNR distribution can improve the detection performance of diversity radar. Whether certain channel SNRs can achieve a higher optimal detection probability than another depends on total channel SNR and false alarm rate.

I. INTRODUCTION

Inspired by the achievements in multiple-input multiple-output (MIMO) communication, the MIMO concept was generalized into the radar field in [1], which has then rapidly drawn considerable attention [2–6]. In terms of the spacing between its antennas, MIMO radar is categorized into two types [6], colocated MIMO radar [4, 7, 8] and distributed MIMO radar [2, 9]. Colocated MIMO radar can increase parameter identifiability of radar targets [10, 11] and can adaptively suppress more inactive point interferences [8, 12], compared with its phased-array radar counterpart with the same number of antennas. Distributed MIMO radar is actually a kind of multistatic radar or multisite radar systems, which have been intensively studied earlier in [13]. The relationship between distributed MIMO radar and multisite radar systems was analyzed in [5]. As shown in [6, 13], multisite radar systems have many known advantages in comparison with conventional monostatic radars, such as expanded coverage, better detection performance, higher target localization accuracy and better jamming cancellation performance (see also [2, 13, 14]).

Distributed MIMO radar is also termed spatial diversity MIMO radar [13] because it can exploit target spatial scattering diversity to combat target radar cross section (RCS) scintillation. Besides spatial scattering diversity, radar targets also bear frequency scattering diversity, i.e., a radar target may reflect different responses when illuminated by signals of different carrier frequencies. Target frequency scattering diversity can also be used to combat target RCS fluctuation [15, 16]. In spatial-frequency joint diversity radar (SFDR) [17] which contains multiple widely separated radar sites all capable of working at multiple frequencies, both spatial scattering diversity and frequency scattering diversity of radar targets can be exploited. Using the incoherent accumulating detection (IAD) algorithm with uniform weights, it was found that both spatial diversity radar [13] and frequency diversity radar [15, 16, 18] can achieve a better detection performance than a nondiversity one.

However, for distributed MIMO radar, it is often difficult for the IAD with uniform weights to reach the optimal detection performance because of two challenges. The first is that radar sites in an SFDR may have different channel signal-to-noise ratios (SNRs) for many reasons, such as different distances from radar sites to a target. The second is that complex envelopes of target returns in diversity channels may be partially correlated [17]. In order to realize the potentials of diversity radar in detection performance, high-performance detection algorithms should be designed.

For conventional monostatic radar, the above-mentioned two challenges may be circumvented by properly choosing radar parameters. In this case, the classical Swerling model [19], which simply deems complex envelopes of target returns either completely correlated or independent, can be used with an acceptable

detection performance loss. The Swerling model was also used early in [13] and later in [2, 20, 21] to evaluate the detection performance of distributed MIMO radar. The Swerling model was actually proposed for conventional radar and one should be careful when generalizing it to distribution MIMO radar, especially for some situations where target returns are partially correlated.

In fact, it has been noticed that several kinds of diversity radar may received partially correlated target returns [17, 22]. In this case, it may be unreasonable to deem target returns either completely correlated or statistically independent. For partially correlated target returns, correlation coefficient is widely used as a measure of correlation of target returns. For instance, in both conventional nondiversity radar [23] and emerging distributed MIMO radar [24, 25], correlation coefficient is used to describe the degree of correlation of target returns. However, the correlation coefficient was derived for certain simple situations in [23–25] and the resulting correlation coefficients are powers of a seed correlation coefficient. In some situations, both the seed correlation coefficient and the powers may be difficult to determine. In diversity radar with complicated structures, such as the SFDR, this target model may no longer be applicable.

For distributed MIMO radar, the correlation of target returns depends on where the target is present [22, 25, 26]. No matter how far radar sites are spatially separated, provided that the angles of view of radar sites to a target are sufficiently close, partially correlated target returns will be received [17, 22]. In order to study spatial diversity and frequency diversity of radar targets in a uniform framework, correlation coefficient of target returns is formulated at the background of an SFDR system in [17]. The SFDR contains multiple kinds of diversity channel pairs. Some diversity channel pairs are present in spatial diversity radar and frequency diversity radar, while some diversity channels are untouched before, such as the diversity channel pair of which two diversity channels have different transmitters, different receivers, and different working frequencies. The diversity channel pairs are categorized into four types. For all types of diversity channel pairs in the SFDR, based on a round-shaped scatterers center target model, it is proved that the correlation coefficient of two target returns can be expressed by a function of target size and the correlation of two channels. The correlation of two channels is measured by the equivalent frequency interval (EFI). Different types of diversity channel pairs have different expressions of the EFI [17]. This method directly calculates correlation coefficients of target returns in diversity channels and enables the design of novel detection algorithms for diversity radars involving both spatial diversity and frequency diversity.

In this paper, we first briefly introduce the method proposed in [17] to estimate correlation coefficient of target returns in the SFDR. In association with channel SNRs, a target fluctuation covariance matrix (TFCM) is defined. According to channel SNR distribution and correlation of target returns, six typical situations regarding channel SNR distribution and correlation of target returns are considered, each bearing certain distinct structures of the TFCM. Based on the Neyman-Pearson criterion [27], several detection algorithms are formulated with respect to the situations. For instance, the general Gaussian signal detector (GGSD) is formulated for the situation where the TFCM is an arbitrary semidefinite positive Hermitian matrix; the SNR weighting based detector (SWD) is formulated for the situation where the TFCM can be considered as a diagonal matrix.

In practice, the presumed TFCM structure may mismatch the real one. Meanwhile, the unknown parameters used to compute the TFCM may be estimated in low accurancy. In this case, the resulting detection algorithms may suffer from a detection performance loss. Therefore, we derive theoretical detection probabilities of concerned detection algorithms when the TFCM takes any possible structure.

The detection performances of concerned detection algorithms are analyzed via numerical results in several different scenarios. We first study the impact of target correlation coefficient and channel EFI on target detection performances of concerned detection algorithms and the diversity radar itself. Then we concern a situation where target returns are statistically independent but channel SNRs are different. Finally, a diversity radar system with more diversity channels is considered, where target returns are partially correlated and channel SNRs are different.

Using the GGSD with exact knowledge of statistical distribution of target returns, the optimal detection performance of diversity radar is studied when target returns are partially correlated and channel SNRs are different. It is found that whether a diversity radar would bear a higher detection performance than that of a nondiversity one depends on both the total SNR of diversity channels and the false alarm rate prescribed. Given total SNR and false alarm rate, only an appropriate degree of signal diversity can achieve the highest detection probability. As special cases of the SFDR, most existing spatial diversity radar and frequency diversity radar can share the same results and conclusions presented in this work.

The rest of this paper is organized as follows. Section II introduces the SFDR concerned in [17] and the method to estimate target correlation coefficients. In Section III, we formulate target detection algorithms for six typical radar situations, different in assumptions imposed on the correlation of target returns and channel SNR distribution. Via numerical results, Section IV studies the detection performances of detection algorithms and diversity radar itself when target returns are partially correlated and channel SNRs are different. Section V presents conclusions and discussion.
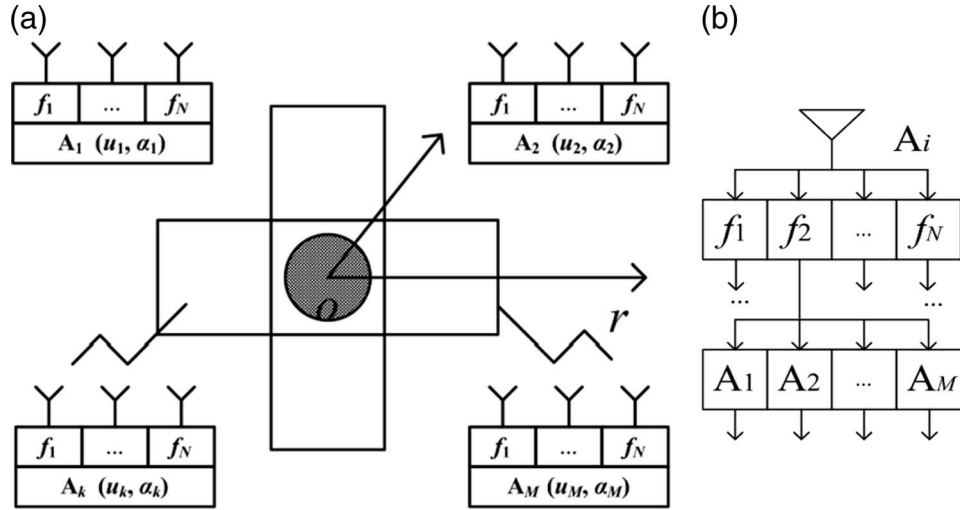
Fig. 1. (a) Topology of SFDR system. (b) Diversity receiving channels in receiving end of radar site.

II. SFDR and TFCM

A. Deployment of the SFDR

The topology of the SFDR system concerned in [17] is shown in Fig. 1(a), where A_i, $i = 1, 2, \cdots$ denote spatially distributed radar sites, the squares stand for spatial resolution cells, the square with a shadowed circle inside represents the spatial resolution cell under test, and the shadowed circle represents a possible radar target. For simplicity, assume that working frequencies of the radar sites are chosen from the same set. Each radar site has an identity code to modulate its transmit waveforms. The identity codes are orthogonal to each other [28], and the orthogonality between the identity codes is maintained even for different mutual delays, such that a receiver can distinguish received signals caused by different transmitters. A low degree of correlation between waveforms can avoid mutual interference between signals transmitted by different radar sites but of the same carrier frequency. Ideal orthogonality even at different mutual delays is nearly impossible for real waveforms and there are many algorithms proposed to design waveforms for MIMO radar [28, 29].

At the receiving end of each radar site, returns due to different transmitters should be separated. For the SFDR under consideration, there are various signal processing schemes to separate returns due to different transmitters. A typical one is given in Fig. 1(b), which is proposed in [17]. In this signal processing scheme, received signals would first pass a filter bank composed of filters working at different frequencies to separate the returns of different carrier frequencies. Subsequently, the output signals of such a filter would then pass another filter bank composed of filters whose weights are the identity codes, such that the returns of the same frequency but from different transmitters can be separated. At this stage, the identity codes are actually used to distinguish target returns caused by different transmitters. This process can be considered

as matched filtering or range compression. At the output of this process, the returns due to different transmitters can be finally separated.

Assume that transmit waveforms are narrowband and their range resolutions are all greater than target size. After range compression, a range cell is sufficient to accommodate a target return. For the spatial resolution cell under test, each active diversity channel can contribute an observation or a sample, which would be transmitted to the signal fusion center to make a global decision on whether a target is present in the spatial resolution cell or not.

B. Target Detection Problem for Diversity Radar

Assume that at the fusion center, L observations from L active diversity channels with respect to a spatial resolution cell under test are available, denoted by $\mathbf{r} \in C^{L \times 1}$. In the spatial resolution cell under test, a target is either present or absent and thus the observations $\mathbf{r}$ under both the hypotheses can be written as

$$\begin{cases} \mathbf{r} = \mathbf{n}, & H_0 : \text{ Target is absent} \\ \mathbf{r} = \mathbf{s} + \mathbf{n}, & H_1 : \text{ Target is present} \end{cases} \tag{1}$$

where $\mathbf{s} \in C^{L \times 1}$ is a vector of the returns from a target possibly present in the spatial resolution cell under test, and $\mathbf{n} \in C^{L \times 1}$ is the channel interference component.

Before introducing the method to estimates correlation coefficients of target fluctuations in diversity channels, we first state the necessity to estimate them in the radar target detection problem. According to the Neyman-Pearson criterion [30], the detection algorithm with the optimal detection performance can be developed using the following likelihood ratio test

$$\Lambda(\mathbf{r}) = \frac{f_{\mathbf{r}|H_1}(\mathbf{r})}{f_{\mathbf{r}|H_0}(\mathbf{r})} \underset{H_0}{\overset{H_1}{\gtrless}} \delta \tag{2}$$

where δ denotes a threshold, and $f_a(\cdot)$ denotes the probability distribution function (pdf) of a random variant a.

It can be seen from the test (2) that the statistical distribution of received signals under both the hypotheses are indispensible to derive the optimal detection algorithm. Generally speaking, target returns are statistically independent of background interference signals. So we have to obtain the statistical distribution of **s** for obtaining $f_{\mathbf{r}|H_1}(\mathbf{r})$.

In practice, targets falling into the scope of a radar may be of various types. Different targets have different scattering characteristics. Therefore, it is very difficult to find a target model matching all possible targets. In the radar field, one often uses a mathematically tractable replacement of possible targets, based on which the statistical distribution of **s** can be formulated.

The scatterers center target model is a widely used replacement to approximate the scattering characteristic of possible radar targets [2, 13, 26, 31]. According to this target model, a radar target is composed of multiple scattering centers with statistically independent scattering intensities and then a target return is simply a sum of responses of those scattering centers. For multisite radar systems, this target model is used in [13] to derive the so-called space-time correlation matrix of signal fluctuations.

As a sum of many statistically independent elements, the target return component is often considered as a random variable following a zero-mean complex Gaussian distribution. Under the narrowband assumption on transmit waveforms, the target return component can be considered to be in a spatial resolution cell. In order to obtain the statistical distribution of **s**, the TFCM is indispensible.

Radar detection algorithms are often designed under a specific assumption on the structure of the TFCM. For instance, for conventional nondiversity radar, target returns are often assumed to be completely correlated and then the elements of the TFCM have the same modulus; while for frequency diversity radar, target returns are often assumed to be statistically independent and then the TFCM is reduced to a diagonal matrix with identical diagonal elements.

For the SFDR at hand, it is difficult to make envelopes of target returns from all active diversity channels statistically independent [26]. Therefore, in the case of the SFDR, the correlation of target returns is much more complicated. Target returns may be neither completely correlated nor independent and then the TFCM may exhibit structures that are more complicated. In this case, it may be inappropriate to impose a specific structure on the TFCM and thus its elements should be estimated separately.

C. Correlation Coefficient of Target Returns

Under the H_1 hypothesis, the signal received in the ith active diversity channel with respect to the resolution cell under test can be rewritten as [17]

$$r_i = s_i + n_i, i = 1, \ldots, L \qquad (3)$$

where n_i denotes the channel interference component,

$$s_i = \sqrt{E_i}\eta_i \exp(-j2\pi f_i D_i/\mathrm{c}) \qquad (4)$$

the target response component, $\sqrt{E_i}\eta_i$ denotes the envelope of the target return, E_i denotes the variance or mean power of the target response component, η_i denotes the target scattering fluctuation term, f_i denotes the working frequency of the ith diversity channel, D_i denotes the distance from the transmitter to the target center and then back to the receiver, and c denotes the speed of light. The envelope of target return is modeled as a zero-mean complex Guassian distributed variable, so E_i stands for its variance and η_i is a normalized random variable following the standard complex Gaussian distribution.

For diversity radar, independent target components are preferable, because the optimal detection algorithm for them has a simple structure and a low computation cost. Independence criterion is a criterion to assess whether $\eta_i, i = 1, 2, \ldots$ are statistically independent. Independence criteria for distributed MIMO radar and frequency diversity radar have been studied in the past [2, 13, 15, 16]. For instance, the spatial-temporal correlation matrix of signal envelopes from an arbitrary 3D moving target is derived in [13] for distributed radar. In addition, simple approximate equations and inequalities are given in [13] for regions of high and low correlation. For the SFDR under consideration, a unified independence criterion for any kind of diversity channel pairs is proposed in [17] as

$$f_\mathrm{e}d/\mathrm{c} \geq \varepsilon/2 \qquad (5)$$

where d denotes target size, ε is a strictness factor commonly set by $\varepsilon = 1$ [1, 2, 15, 16], and f_e denotes the EFI of a diversity channel pair defined in [17]. In [17], a polar coordinate system was constructed with its origin located at target center. For the diversity channel with respect to the ith sample, the polar angle of its transmitter is denoted by α_i, and that of its receiver by β_i. The EFI of the diversity channel pair composed of the ith and the jth diversity channel can be expressed by [17]

$$\begin{aligned}
f_\mathrm{e} = \frac{1}{2}\mathrm{sqrt}\Big\{&2f_i^2\left[1 + \cos(\alpha_i - \beta_i)\right] \\
&+ 2f_j^2\left[1 + \cos(\alpha_j - \beta_j)\right] \\
&- 2f_i f_j\big[\cos(\alpha_i - \alpha_j) + \cos(\alpha_i - \beta_j) \\
&+ \cos(\beta_i - \alpha_j) + \cos(\beta_i - \beta_j)\big]\Big\}
\end{aligned} \qquad (6)$$

where $\mathrm{sqrt}(\cdot)$ denotes the square root.

For distributed MIMO radar, the noncoherent signal processing scheme is less difficult to implement in a real engineering application than the coherent processing scheme. In order to make the noncoherent signal processing scheme achieve a better detection performance, target returns received by widely separated radar sites should be statistically independent. For that purpose,

relative working parameters of distributed MIMO radar are often designed to meet a certain independence criterion.

However, an independence criterion cannot tell the degree of correlation of partially correlated target returns. As it is often difficult in practice to totally exclude partially correlated target returns [17, 26], accurate description of the correlation of target returns is critical for distributed MIMO radar that may receive partially correlated target returns. Based on the round-shaped scatterers center target model, a unified expression of the correlation coefficient was developed for all kinds of diversity channel pairs present in the SFDR. Specifically, the correlation coefficient of the envelopes of two target returns from the ith and the jth diversity channel of the SFDR can be expressed by [17]

$$\rho = \mathrm{E}\left(\eta_i \eta_j^*\right) = \mathrm{jinc}\left(2 f_e d/c\right) \tag{7}$$

where $\mathrm{E}\left(\cdot\right)$ is the expectation operation,

$$\mathrm{jinc}\left(x\right) = 2\mathrm{J}_1\left(\pi x\right)/\pi x \tag{8}$$

is known as the "jinc" function in optical literature [32], and $\mathrm{J}_1\left(\cdot\right)$ is the Bessel function of the first kind of the first order.

This result can be applied not only to the SFDR under consideration but also to most radars involving spatial diversity and frequency diversity, whose diversity channels are all included in the SFDR as well (see [17] for details).

As a measurement of correlation coefficient, $|\rho| \leq 1$. Theoretically speaking, if $|\rho| = 1$, target fluctuations can be considered to be completely correlated; if $0 < |\rho| < 1$, target fluctuations can be considered to be partially correlated; if $\rho = 0$, target fluctuations can be considered to be statistically independent. However, as shown in [17], the correlation coefficient with respect to the independence criterion is actually not zero but 0.1812 instead. Therefore, the independence criterion is just a convention, not a strict value.

The effect of target movement on target fluctuation is developed in [13] but is not considered in the derivation in [17], for that the coordinate system used in [17] for derivation is fixed on the target and thus the motion of target is transferred to the motion of radar sites. In fact, the fluctuation of target returns for a moving target is caused by the spatial diversity of the target. Given a radar system and its probing waveform, a stationary target in space would theoretically always give the same response whenever we probe it. Therefore, target temporal fluctuation is essentially a kind of target spatial fluctuation. With this fact in mind, one can analyze the impact of target movement under this framework as well. This problem will not be addressed further here for simplicity.

D. TFCM

From (7), correlation coefficient of target returns depends on both target size represented by d and channel correlation measured by f_e. For each spatial resolution cell, its spatial location can be estimated via time of arrival

and direction of arrival and then the channel correlation measure f_e can be calculated with great accuracy.

In estimation of correlation coefficients of target returns, target size d is more difficult to determine than the f_e, because real targets often have different sizes and thus may give responses with different correlation characteristics. The choice of target size is discussed later and we first assume that target size has been predetermined according to a certain criterion.

Based on a given target size, the correlation coefficients of target returns can be estimated according to (7). For all active diversity channels in SFDR, the correlation coefficients of target returns can comprise a matrix denoted by $\boldsymbol{\Theta}_t = E\left(\boldsymbol{\eta}\boldsymbol{\eta}^{\mathrm{H}}\right)$, where $\boldsymbol{\eta} = [\eta_1, \ldots, \eta_L]^{\mathrm{T}}$, $(\cdot)^{\mathrm{H}}$ denotes the conjugate transpose and $(\cdot)^{\mathrm{T}}$ denotes the transpose. It can be proved that $\boldsymbol{\Theta}_t$ is a Hermitian matrix. Its diagonal elements are all ones, and the others have absolute values less than or equal to one. Taking the range phase term into consideration, we can define a signal correlation coefficient matrix by

$$\boldsymbol{\Theta}_s = \mathrm{diag}\left(\mathbf{p}\right) \boldsymbol{\Theta}_t \mathrm{diag}\left(\mathbf{p}^*\right) \tag{9}$$

where

$$\mathbf{p} = \left[\exp\left(-j2\pi f_1 D_1/c\right), \ldots, \exp\left(-j2\pi f_L D_L/c\right)\right]^{\mathrm{T}}$$

is an $L \times 1$ vector of the channel range phase terms, $\mathrm{diag}\left(\mathbf{p}\right)$ with a vector entry stands for a diagonal matrix with the entry vector $\mathbf{p}$ as its diagonal elements, and $(\cdot)^*$ denotes the conjugate. Based on the signal correlation coefficient matrix $\boldsymbol{\Theta}_s$, the signal covariance matrix can be defined by

$$\mathbf{C}_s = \mathrm{E}\left(\mathbf{s}\mathbf{s}^{\mathrm{H}}\right) = \mathrm{diag}\left(\mathbf{E}\right) \mathrm{diag}\left(\mathbf{p}\right) \boldsymbol{\Theta}_t \mathrm{diag}\left(\mathbf{p}^*\right) \mathrm{diag}\left(\mathbf{E}\right) \tag{10}$$

where $\mathbf{E} = \left[\sqrt{E_1}, \ldots, \sqrt{E_L}\right]^{\mathrm{T}}$.

For coherent signal processing algorithms, the range phase term $\mathbf{p}$ generally has a great impact on the target detection performance. Only under the condition that the range phase terms can be perfectly compensated in each diversity channel, can coherent signal processing algorithms reach their best detection performance. Therefore, range phase compensation is an important issue. In this work however, we are concerned more about correlation of target returns and the distribution of channel SNRs, because both of them have a great impact on the optimal detection performance. Therefore, we simply assume that the range phases of diversity channels are exactly known and thus can be perfectly compensated.

Excluding the range phase term $\mathbf{p}$, the covariance matrix of target fluctuations (TFCM) can be defined by

$$\mathbf{C}_t = \mathrm{diag}\left(\mathbf{E}\right) \boldsymbol{\Theta}_t \mathrm{diag}\left(\mathbf{E}\right) \tag{11}$$

The relationship between $\mathbf{C}_s$ and $\mathbf{C}_t$ is

$$\mathbf{C}_s = \mathrm{diag}\left(\mathbf{E}\right) \boldsymbol{\Theta}_s \mathrm{diag}\left(\mathbf{E}\right) = \mathrm{diag}\left(\mathbf{p}\right) \mathbf{C}_t \mathrm{diag}\left(\mathbf{p}^*\right). \tag{12}$$

The interference covariance matrix is denoted by $\mathbf{C}_n = \mathrm{E}\left(\mathbf{n}\mathbf{n}^{\mathrm{H}}\right)$. It can be easily proved that $\mathbf{C}_n$, $\boldsymbol{\Theta}_t$, $\boldsymbol{\Theta}_s$, $\mathbf{C}_t$, and $\mathbf{C}_s$ are all positive semidefinite matrices.

The eigen decomposition of the TFCM $\mathbf{C}_t$ can be written as

$$\mathbf{C}_t = \mathbf{Q}_t \mathbf{\Lambda}_t \mathbf{Q}_t^H \qquad (13)$$

where $\mathbf{Q}_t$ takes the eigenvectors as its columns, $\mathbf{\Lambda}_t = \mathrm{diag}\,(\mathbf{h}_t)$, and $\mathbf{h}_t = [h_1, \ldots, h_L]^T$ is a vector of the eigenvalues. Since $\mathbf{C}_t$ is positive semidefinite, without loss of generality, we assume that the eigenvalues in $\mathbf{h}_t$ are sorted in a descending order such that $h_1 \geq \cdots \geq h_L \geq 0$. From (12) and (13), $\mathbf{C}_s$ can be decomposed into

$$\mathbf{C}_s = \mathrm{diag}\,(\mathbf{p})\,\mathbf{Q}_t \mathbf{\Lambda}_t \mathbf{Q}_t^H \mathrm{diag}\,(\mathbf{p}^*) \qquad (14)$$

where $\mathrm{diag}\,(\mathbf{p})\,\mathbf{Q}_t$ takes the eigenvectors of $\mathbf{C}_s$ as its columns.

The method to estimate correlation coefficients of target returns has been presented. In addition to estimates of interference distribution and channel SNRs, the pdfs of received signal under both of the hypotheses can be obtained and then detection algorithms can be formulated from the likelihood ratio test (2), as shown subsequently.

III. DETECTION ALGORITHMS FOR DIVERSITY RADAR

In this section, we first formulate the detection algorithm when TFCM is exactly known. Then how to estimate the TFCM is discussed. In some situations, the TFCM may take a special structure and according to the structure of the TFCM, six typical situations are considered, based on which corresponding detection algorithms are formulated.

A. Detection Algorithm for General Cases

Assume that the background interferences in diversity channels follow zero-mean complex Gaussian distribution with covariance matrix $\mathbf{C}_n = E\,(\mathbf{nn}^H)$. Under the H_0 hypothesis, the covariance matrix of $\mathbf{r}$ under the H_0 hypothesis can be written as

$$\mathbf{C}_0 = \mathrm{E}\,(\mathbf{rr}^H \,|\, H_0) = \mathrm{E}\,(\mathbf{nn}^H) = \mathbf{C}_n. \qquad (15)$$

The pdf $f_{\mathbf{r}|H_0}\,(\mathbf{r})$ can be expressed as follows

$$\begin{aligned} f_{\mathbf{r}|H_0}\,(\mathbf{r}) &= \frac{1}{\pi^L \,|\mathbf{C}_0|} \exp\left(-\mathbf{r}^H \mathbf{C}_0^{-1} \mathbf{r}\right) \\ &= \frac{1}{\pi^L \,|\mathbf{C}_n|} \exp\left(-\mathbf{r}^H \mathbf{C}_n^{-1} \mathbf{r}\right) \qquad (16) \end{aligned}$$

where $|\cdot|$ with a square matrix entry denotes the determinant of the entry matrix.

Under the assumption that target returns and channel interferences are statistically independent of each other, the covariance matrix of $\mathbf{r}$ under the H_1 hypothesis, denoted by $\mathbf{C}_1$, can be written as $\mathbf{C}_1 = \mathrm{E}\,(\mathbf{rr}^H \,|\, H_1) = \mathbf{C}_s + \mathbf{C}_n$. Therefore, the pdf $f_{\mathbf{r}|H_1}\,(\mathbf{r})$ can be expressed by

$$\begin{aligned} f_{\mathbf{r}|H_1}\,(\mathbf{r}) &= \frac{1}{\pi^L \,|\mathbf{C}_1|} \exp\left(-\mathbf{r}^H \mathbf{C}_1^{-1} \mathbf{r}\right) \\ &= \frac{1}{\pi^L \,|\mathbf{C}_s + \mathbf{C}_n|} \exp\left[-\mathbf{r}^H (\mathbf{C}_s + \mathbf{C}_n)^{-1}\,\mathbf{r}\right]. \qquad (17) \end{aligned}$$

Inserting pdfs (16) and (17) into (2) and after some simple manipulations, we can obtain the following test statistic [30]

$$T\,(\mathbf{r}) = 2\mathbf{r}^H \left(\mathbf{C}_0^{-1} - \mathbf{C}_1^{-1}\right) \mathbf{r} = 2\mathbf{r}^H \Delta \mathbf{C}\mathbf{r} \qquad (18)$$

where

$$\Delta\mathbf{C} = \mathbf{C}_0^{-1} - \mathbf{C}_1^{-1} = \mathbf{C}_n^{-1} - (\mathbf{C}_s + \mathbf{C}_n)^{-1}. \qquad (19)$$

Derived from the Neyman-Pearson criterion, the test statistic (18) is optimal if all the involved parameters, i.e., $\mathbf{C}_n$ and $\mathbf{C}_s$, are exactly known.

In practice, if background interference contains only the channel thermal noise, the interference covariance matrix $\mathbf{C}_n$ can be considered as an identity matrix after normalization of received signals with respect to noise levels of diversity channels. If clutter returns are present in frequency diversity channels or jamming signals are present in spatial diversity channels, the interferences with respect to the same resolution cell may be mutually correlated and then $\mathbf{C}_n$ may no longer be an identity matrix. In this case, if we estimate $\mathbf{C}_n$ by using some independent and identically distributed training samples, the detection algorithm resulted from (18) does not bear the constant false-alarm rate (CFAR) property with respect to $\mathbf{C}_n$. Therefore, we do not consider a detection algorithm for this situation.

However, if training samples are sufficient to obtain an ideal estimate of $\mathbf{C}_n$, with a linear transform $\mathbf{C}_n^{-1/2}\mathbf{r}$ to received signals $\mathbf{r}$, the resulting interference covariance matrix $\mathbf{C}_n$ becomes an identity matrix $\mathbf{I}$. After this transformation, the signal covariance matrix becomes $\mathbf{C}_n^{-1/2}\mathbf{C}_s\mathbf{C}_n^{-1/2}$, which can be proved to still be a positive semidefinite Hertimian matrix as $\mathbf{C}_s$. Therefore, without loss of generality, we always assume in what follows that $\mathbf{C}_n = \mathbf{I}$ and still denote the signal covariance matrix by $\mathbf{C}_s$. In this case, we have

$$\begin{cases} \mathrm{E}\,(\mathbf{r}\,|\,H_0) = 0 \\ \mathbf{C}_0 = \mathrm{E}\,(\mathbf{rr}^H \,|\,H_0) = \mathbf{C}_n = \mathbf{I} \end{cases} \qquad (20)$$

and

$$\begin{cases} \mathrm{E}\,(\mathbf{r}\,|\,H_1) = 0 \\ \mathbf{C}_1 = \mathrm{E}\,(\mathbf{rr}^H \,|\,H_1) = \mathbf{I} + \mathbf{C}_s \end{cases} \qquad (21)$$

For the target component s_i, we define the SNR for such a random value with respect to the ith diversity channel by

$$E_i = \frac{\mathrm{var}\,(s_i)}{\mathrm{var}\,(n_i)}. \qquad (22)$$

In the numerical experiment section, the concept of total SNR (TSNR) will be used to measure the detection performance of diversity radars, which is defined by

$$\mathrm{TSNR} = \sum_{i=1}^{L} E_i = \sum_{i=1}^{L} \frac{\mathrm{var}\,(s_i)}{\mathrm{var}\,(n_i)}. \qquad (23)$$

TABLE I
Six Typical Situations Regarding Channel SNR Distribution and Correlation of Target
Returns

Channel SNR Distribution	Correlation of Target Returns		
	Completely Correlated	Independent	Partially Correlated
Uniform	I	II	III
Nonuniform	IV	V	VI

If the noise levels of all diversity channels are identical, we have

$$\text{TSNR} = \frac{\sum_{i=1}^{L} \text{var}\,(s_i)}{\text{var}\,(n)}. \tag{24}$$

Therefore, given a TSNR, the total power of target components in received signals can be considered as a constant, hence the name TSNR. Using the TSNR, a fair comparison of the detection performance between diversity radars with SNR ratios can be guaranteed.

Under the assumption that the channel range phase terms are known a priori, the parameters left unknown to construct the TFCM are the correlation coefficient matrix $\boldsymbol{\Theta}_t$ and the channel SNR vector $\mathbf{E}$. In certain scenarios, the TFCM may take some special structures and the structure is mainly determined by $\boldsymbol{\Theta}_t$ and $\mathbf{E}$. Based on possibilities of $\boldsymbol{\Theta}_t$ and $\mathbf{E}$, we categorize real situations into six different scenarios, which are listed in Table I.

In Table I, "completely correlated" means that $\boldsymbol{\Theta}_t$ is an all-one matrix; "independent" means that $\boldsymbol{\Theta}_t$ is an identity matrix; "semicorrelated" means that $\boldsymbol{\Theta}_t$ may be any kind of correlation coefficient matrix of envelopes of target returns; "uniform" means that all the elements in $\mathbf{E}$ are the same; "nonuniform" means that the elements in $\mathbf{E}$ may be different.

It should be noted that four among six situations (i.e., I, II, IV, and V) have been considered before in [13] while the two left (i.e., III and VI) have seldom been considered.

In these scenarios, there are some statistical distribution parameters unknown and needing for estimation. The accuracy of the estimation has a great impact on the detection performance of the resulting detection algorithms. Therefore, in the following, we first discuss how to estimate them in engineering practice.

B. Estimation of TFCM

The TFCM is computed by $\boldsymbol{\Theta}_t$ and $\mathbf{E}$, both needed for estimation. As mentioned above, target size has a great impact on the degrees of statistical correlation of target returns. However, online estimation of signal correlation is not suggested at the target detection stage, because at this stage, we do not know whether a target is present in the spatial resolution cell, not to mention its shape and size. Furthermore, even if a target is present, the SNR may be low and the sample size may be limited, making the estimation possibly inaccurate. For the same reason, it is not recommended to estimate $\mathbf{E}$ by online real data as well.

We first consider the estimation of $\boldsymbol{\Theta}_t$. We recommend to estimate the target size parameter offline instead of online. According to formula (7), the target correlation coefficient depends on two factors: one is the channel correlation indicated by the EFI f_e, and the other is the target size indicated by d. From (6), the EFI may depend on both radar working frequency (or frequencies) and the spatial location of the presumed target. Given a deployment of radars, one can accurately calculate an EFI for any spatial resolution cell with great accuracy according to (6). The spatial location of a spatial resolution cell can be generally determined by time of arrival and direction of arrival of received signals. A spatial resolution cell generally occupies a certain area and one can calculate the EFI with respect to its center. The spatial points within a spatial resolution cell may give rise to different EFIs, but if the size of the spatial resolution cell is far smaller than the distance between radar sites and the center of the spatial resolution cell, the EFIs of the spatial points are often close to each other. Therefore, spatial points in the same spatial resolution cell can be considered to bear the same EFI.

The difficulty of the correlation coefficient estimation lies in the way to select the target size. If target size can be accurately estimated, the resulting detection algorithm would be close to the optimal one; larger target-size mismatch may result in a greater loss in detection performance. Real targets may have any shape, size, and attitude. A target size matching a group of targets may mismatch others and thus it is very difficult to match all possible targets perfectly.

Fortunately, targets of interest to a real radar system, such as planes and missiles, often have a limited range of size. Based on this knowledge, one can choose the most common target size, the size of the most valuable targets, the statistical average of the sizes of possible targets, or values determined by other criteria. In accordance to whatever criterion, one can determine a target size and we denote it here by $\hat{d}$, in expectation that the detection performance loss is acceptable.

With the EFI calculated and target size estimated or presumed, a target correlation coefficient matrix can be estimated offline for any spatial resolution cell. For the spatial resolution cell under test, the estimate of target correlation coefficient matrix is denoted by $\hat{\boldsymbol{\Theta}}_t$ and the estimate of channel SNRs by $\hat{\mathbf{E}}$. With $\hat{\boldsymbol{\Theta}}_t$ and $\hat{\mathbf{E}}$ at hand, an estimate of $\mathbf{C}_t$ can be obtained as

$$\hat{\mathbf{C}}_t = \text{diag}\left(\hat{\mathbf{E}}\right) \hat{\boldsymbol{\Theta}}_t \text{diag}\left(\hat{\mathbf{E}}\right). \tag{25}$$

Because $\boldsymbol{\Theta}_t$ is a positive semidefinite Hermitian matrix, its estimate $\hat{\boldsymbol{\Theta}}_t$ should be guaranteed to be positive semidefinite Hermitian matrix as well. If $\hat{\boldsymbol{\Theta}}_t$ obeys this condition, $\hat{\mathbf{C}}_t$ and $\hat{\mathbf{C}}_s = \mathrm{diag}\,(\mathbf{p})\,\hat{\mathbf{C}}_t\mathrm{diag}\,(\mathbf{p})$ obey as well. The eigen decomposition of $\hat{\mathbf{C}}_t$ can be expressed by

$$\hat{\mathbf{C}}_t = \hat{\mathbf{Q}}_t\mathrm{diag}\left(\hat{\mathbf{h}}_t\right)\hat{\mathbf{Q}}_t^H \qquad (26)$$

where $\hat{h}_1, \ldots, \hat{h}_L$ are eigenvalues of $\hat{\mathbf{C}}_t$, and $\hat{\mathbf{Q}}_t$ is a matrix of eigvenvectors. Without loss of generality, we assume that $\hat{h}_1 \geq \hat{h}_2 \geq \cdots \geq \hat{h}_L \geq 0$. The rank of $\hat{\mathbf{C}}_t$, denoted by N_r, satisfies $N_r \leq L$. The optimal detection algorithm in (18) uses the real parameters of the statistical distribution of received signals under two hypotheses. In practice, those distribution parameters should be replaced by estimated values or presumed ones. In the following, under different presumptions on those unknown parameters, we derive different target detection algorithms.

C. GGSD

1) *Test Statistic*: In situation VI, all the parameters are unknown and thus should be estimated. Substituting $\hat{\mathbf{C}}_s$ for $\mathbf{C}_s$ in (18), we have

$$T\,(\mathbf{r}) = 2\mathbf{r}^H\left[\mathbf{I} - \left(\mathbf{I} + \hat{\mathbf{C}}_s\right)^{-1}\right]\mathbf{r} = 2\mathbf{r}^H\hat{\mathbf{C}}_s\left(\mathbf{I} + \hat{\mathbf{C}}_s\right)^{-1}\mathbf{r} \qquad (27)$$

where

$$\hat{\mathbf{C}}_s = \mathrm{diag}\,(\mathbf{p})\,\hat{\mathbf{C}}_t\mathrm{diag}\,(\mathbf{p}^*) \qquad (28)$$

because $\mathbf{p}$ is known a priori by assumption. According to (28), the test statistic (27) can also be reformulated to

$$T\,(\mathbf{r}) = 2\mathbf{r}^H\mathrm{diag}\,(\mathbf{p})\,\hat{\mathbf{C}}_t\left(\mathbf{I} + \hat{\mathbf{C}}_t\right)^{-1}\mathrm{diag}\,(\mathbf{p}^*)\,\mathbf{r}. \qquad (29)$$

We deem the operation $\mathrm{diag}\,(\mathbf{p}^*)\,\mathbf{r}$ as the phase alignment and phase compensation operation for the diversity channels. Using the eigen decomposition of $\hat{\mathbf{C}}_t$ given by (26), we can further obtain the following test statistic

$$T\,(\mathbf{r}) = 2\mathbf{r}^H\mathrm{diag}\,(\mathbf{p})\,\hat{\mathbf{Q}}_t\mathrm{diag}\,(\hat{\mathbf{w}}_t)\,\hat{\mathbf{Q}}_t^H\mathrm{diag}\,(\mathbf{p}^*)\,\mathbf{r} \qquad (30)$$

where $\hat{\mathbf{w}}_t = [w_1, \ldots, w_L]^T$, and $\hat{w}_i = \hat{h}_i/\left(\hat{h}_i + 1\right)$. In (30), the operation $\hat{\mathbf{Q}}_t^H\mathrm{diag}\,(\mathbf{p}^*)\,\mathbf{r}$ transforms the received signals into statistically independent ones and the independence is maintained for both hypotheses, as will be proved later. The $\hat{w}_i$, $i = 1, \ldots, L$, are the weights applied onto those independent signals.

It can be seen from (30) that if $\hat{\mathbf{Q}}_t$ is rank-deficient, some weights may be zeros. With N_r nonzero weights available, the detection algorithm can be written in another form as

$$T\,(\mathbf{r}) = 2\mathbf{r}^H\mathrm{diag}\,(\mathbf{p})\,\hat{\mathbf{Q}}_{N_r}\mathrm{diag}\,(\hat{\mathbf{w}}_{N_r})\,\hat{\mathbf{Q}}_{N_r}^H\mathrm{diag}\,(\mathbf{p}^*)\,\mathbf{r} \qquad (31)$$

where $\hat{\mathbf{w}}_{N_r}$ denotes a vector of the first N_r nonzero elements of $\hat{\mathbf{w}}_t$, and $\hat{\mathbf{Q}}_{N_r}$ denotes the eigenvectors corresponding to the N_r nonzero eigenvalues. The column vectors of $\hat{\mathbf{Q}}_{N_r}$ construct mutually independent signal

spaces with nonzero SNRs. In practice, the signal space and their weights can be calculated offline while the test statistic (31) needs to be calculated online.

2) *False Alarm Rate*: To derive the false alarm rate, we first apply the following linear transform to the received signals

$$\mathbf{y} = \hat{\mathbf{Q}}_t^H\mathrm{diag}\,(\mathbf{p}^*)\,\mathbf{r}. \qquad (32)$$

Then we can rewrite (30) as

$$T\,(\mathbf{r}) = 2\mathbf{y}^H\mathrm{diag}\,(\hat{\mathbf{w}}_t)\,\mathbf{y}. \qquad (33)$$

Under the null hypothesis, from (20), we have

$$\mathrm{cov}\,(\mathbf{y}\,|H_0) = \mathrm{E}\left(\mathbf{y}\mathbf{y}^H\,|H_0\right)$$
$$= \mathrm{E}\left(\hat{\mathbf{Q}}_t^H\mathrm{diag}\,(\mathbf{p}^*)\,\mathbf{r}\mathbf{r}^H\mathrm{diag}\,(\mathbf{p})\,\hat{\mathbf{Q}}_t\,|H_0\right) = \mathbf{I} \qquad (34)$$

where $\mathrm{cov}\,(\cdot)$ denotes the covariance matrix of a vector of random variables. Therefore, the elements of $\mathbf{y}$ are independent and identically distributed random variables following the standard complex Gaussian distribution. It is well known that the modulus square of a zero-mean complex Gaussian distributed variable follows the exponential distribution. Therefore, the test statistic (33) follows the weighted exponential distribution [33] with weighting vector $\hat{\mathbf{w}}_t$, denoted by $E_{\hat{\mathbf{w}}_t}$. Weighted exponential distribution is actually a special case of weighted Chi-square distribution [34].

The false alarm rate of the test statistic (30) can be expressed by

$$p_f = \mathrm{prob}\left(E_{\hat{\mathbf{w}}_t} \geq g\right) = Q\left(g, E_{\hat{\mathbf{w}}_t}\right) \qquad (35)$$

where g denotes the decision threshold, $\mathrm{prob}\,(\cdot)$ denotes the probability operator, and $Q\left(g, E_{\hat{\mathbf{w}}_t}\right)$ denotes the cumulative distribution function (cdf) of the weighted exponential distribution. $Q\left(g, E_{\hat{\mathbf{w}}_t}\right)$ and the false alarm rate can be calculated by using the method proposed in [33]. However, the expression of $Q\left(g, E_{\hat{\mathbf{w}}_t}\right)$ is complicated and for simplicity we do not show it here. Based on the cdf, the decision threshold g can be obtained by a numerical searching procedure in practice.

3) *Probability of Detection*: Under the H_1 hypothesis, we apply another linear transform to the received signals $\mathbf{r}$, i.e.,

$$\mathbf{y} = (\boldsymbol{\Lambda}_t + \mathbf{I})^{-1/2}\,\mathbf{Q}_t^H\mathrm{diag}\,(\mathbf{p}^*)\,\mathbf{r}. \qquad (36)$$

It can be easily proved that $\mathrm{E}\,(\mathbf{y}\,|H_1) = 0$ and

$$\mathrm{cov}\,(\mathbf{y}\,|H_1)$$
$$= \mathrm{E}\left[(\boldsymbol{\Lambda}_t + \mathbf{I})^{-1/2}\,\mathbf{Q}_t^H\mathrm{diag}\,(\mathbf{p}^*)\,\mathbf{r}\mathbf{r}\mathrm{diag}\,(\mathbf{p})\,\mathbf{Q}_t\,(\boldsymbol{\Lambda}_t + \mathbf{I})^{-1/2}\right]$$
$$= \mathbf{I}. \qquad (37)$$

From (36), we have $\mathbf{r} = \mathrm{diag}\,(\mathbf{p})\,\mathbf{Q}_t\,(\boldsymbol{\Lambda}_t + \mathbf{I})^{1/2}\,\mathbf{y}$ and then the test statistic (30) becomes

$$T\,(\mathbf{r}) = 2\mathbf{y}^H\mathbf{G}\mathbf{y} \qquad (38)$$

where

$$\mathbf{G} = (\boldsymbol{\Lambda}_t + \mathbf{I})^{-1/2}\,\mathbf{Q}_t^H\hat{\mathbf{Q}}_t\mathrm{diag}\,(\hat{\mathbf{w}}_t)\,\hat{\mathbf{Q}}_t^H\mathbf{Q}_t\,(\boldsymbol{\Lambda}_t + \mathbf{I})^{1/2}. \qquad (39)$$

Since all the elements of $\hat{\mathbf{w}}$ are nonnegative, $\mathbf{G}$ is a positive semidefinite Hermitian matrix and its eigen decomposition can be written as $\mathbf{G} = \mathbf{U}\text{diag}\,(\mathbf{v})\,\mathbf{U}^{\text{H}}$, where $\mathbf{U}$ is the eigenvector matrix of $\mathbf{G}$ and $\mathbf{v}$ is the vector of its eigenvalues. To derive the distribution of $T\,(\mathbf{r})$ under the H_1 hypothesis, we apply the following linear transform to $\mathbf{y}$ as

$$\mathbf{z} = \mathbf{U}^{\text{H}}\mathbf{y}. \tag{40}$$

Then we have $T\,(\mathbf{r}) = 2\mathbf{z}^{\text{H}}\text{diag}\,(\mathbf{v})\,\mathbf{z}$. From (37), the mean and covariance matrix of $\mathbf{z}$ is $\text{E}\,(\mathbf{z}) = \mathbf{0}$ and $\text{cov}\,(\mathbf{z}) = \mathbf{U}^{\text{H}}\text{E}\,(\mathbf{z}\mathbf{z}^{\text{H}})\,\mathbf{U} = \mathbf{I}$, respectively. Consequently, the test statistic $T\,(\mathbf{r}\,|H_1)$ follows the weighted exponential distribution with weighting vector $\mathbf{v}$, denoted by $E_{\mathbf{v}}$, and the probability of detection can be expressed by

$$p_{\text{d}} = Q\,(g, E_{\mathbf{v}}). \tag{41}$$

With inaccurate estimate of the real value of $\mathbf{C}_{\text{t}}$, the detection probability of the GGSD can be obtained using expression (41).

If $\mathbf{C}_{\text{t}}$ is exactly known, i.e., $\hat{\mathbf{C}}_{\text{t}} = \mathbf{C}_{\text{t}}$, then $\hat{\mathbf{Q}}_{\text{t}} = \mathbf{Q}_{\text{t}}$, $\text{diag}\,(\hat{\mathbf{w}}_{\text{t}}) = \mathbf{\Lambda}_{\text{t}}\,(\mathbf{\Lambda}_{\text{t}} + \mathbf{I})^{-1}$, $\mathbf{G} = \mathbf{\Lambda}_{\text{t}}$, and $\mathbf{v} = \mathbf{h}_{\text{t}}$. In this case, the maximal detection probability of the GGSD can be achieved as

$$p_{\text{dmax}} = Q\,(g, E_{\mathbf{h}_{\text{t}}}). \tag{42}$$

4) *Discussion*: With a matrix inversing operation in the test statistic (29), it appears that the GGSD algorithm is time consuming. However, $\mathbf{C}_{\text{t}}$, the signal space and its associated weights can be estimated offline instead of online in practice. This makes the computational cost of the test statistic (31) affordable for real application.

According to (11), the estimation of $\mathbf{C}_{\text{t}}$ depends on the estimates of $\mathbf{E}$ and $\mathbf{\Theta}_{\text{t}}$, and a total of $L\,(L + 1)\,/2$ unknown parameters are involved. In some scenarios where some of those parameters can be considered to be the same or to have certain special values, the algorithm can be further simplified.

D. SWD

1) *Test Statistic*: In situation V, target returns in all the diversity channels can be considered to be statistically independent, such that the target correlation coefficient matrix $\mathbf{\Theta}_{\text{t}}$ becomes an identity matrix. Consequently, we have $\mathbf{\Theta}_{\text{s}} = \mathbf{Q}_{\text{t}} = \mathbf{I}$ and $\mathbf{C}_{\text{s}} = \mathbf{\Lambda}_{\text{t}} = \text{diag}\,(\mathbf{E}^2)$. Furthermore,

$$\Delta\mathbf{C} = \mathbf{I} - (\mathbf{\Lambda}_{\text{t}} + \mathbf{I})^{-1} = \mathbf{I} - \left[\text{diag}\,(\mathbf{E}^2) + \mathbf{I}\right]^{-1}$$
$$= \mathbf{\Lambda}_{\text{t}}\,(\mathbf{\Lambda}_{\text{t}} + \mathbf{I})^{-1} = \text{diag}\left[\mathbf{E}^2/\,(\mathbf{E}^2 + 1)\right]. \tag{43}$$

Then the test statistic (18) can be formulated to

$$T\,(\mathbf{r}) = 2\mathbf{r}^{\text{H}}\mathbf{\Lambda}r = 2\mathbf{r}^{\text{H}}\text{diag}\left[\mathbf{E}^2/\,(\mathbf{E}^2 + 1)\right]\mathbf{r}. \tag{44}$$

Using the estimate of $\mathbf{E}$, we can obtain the test of the SNR weighting based detection (SWD) algorithm as

follows

$$T\,(\mathbf{r}) = 2\mathbf{r}^{\text{H}}\text{diag}\left[\hat{\mathbf{E}}^2/\,(\hat{\mathbf{E}}^2 + 1)\right]\mathbf{r} = 2\sum_{i=1}^{L}\frac{\hat{E}_i}{\hat{E}_i + 1}\,|r_i|^2 \tag{45}$$

where $|\cdot|$ with a scalar entry denotes the absolute value of the entry scalar.

From (45), the SWD applies different weights to the received signals according to the SNRs of diversity channels. It can be seen from (45) that if the channel SNRs are all far greater than one, all the weights approximate to one, regardless of the values of the channel SNRs; if all the channel SNRs are far less than one, channel weights are approximately equal to the channel SNRs.

It should be noted that a detection algorithm concerning channel SNR difference was considered much earlier in [13] and a detailed analysis regarding SNR difference was also given therein. However, developed under different criteria, these two tests have slightly different weights. In test (45), the weights for the signals from different channels depend only on the channel SNRs, while in [13], more parameters are involved in the weights.

2) *False Alarm Rate*: Under the null hypothesis and from (20), the test statistic (45) follows weighted exponential distribution with weighting vector $\hat{\mathbf{E}}^2/\,(\hat{\mathbf{E}}^2 + 1)$. Therefore, the false alarm rate can be expressed as

$$p_{\text{f}} = Q\left(g, E_{\hat{\mathbf{E}}^2/(\hat{\mathbf{E}}^2+1)}\right). \tag{46}$$

3) *Probability of Detection*: Under the alternate hypothesis, we still apply the linear transform (36) to $\mathbf{r}$ and then obtain

$$T\,(\mathbf{r}) = 2\mathbf{y}^{\text{H}}\underline{\mathbf{G}}\,\mathbf{y} \tag{47}$$

where

$$\underline{\mathbf{G}} = (\mathbf{\Lambda}_{\text{t}} + \mathbf{I})^{1/2}\,\mathbf{Q}_{\text{t}}^{\text{H}}\text{diag}\left[\hat{\mathbf{E}}^2/\,(\hat{\mathbf{E}}^2 + 1)\right]\mathbf{Q}_{\text{t}}\,(\mathbf{\Lambda}_{\text{t}} + \mathbf{I})^{1/2}. \tag{48}$$

Just like $\mathbf{G}$, $\underline{\mathbf{G}}$ is a positive semidefinite Hermitian matrix and can be decomposed as $\underline{\mathbf{G}} = \underline{\mathbf{U}}\text{diag}\,(\underline{\mathbf{v}})\,\underline{\mathbf{U}}^{\text{H}}$, where $\underline{\mathbf{U}}$ is the eigenvector matrix and $\underline{\mathbf{v}}$ is a vector of eigenvalues. With the linear transform $\underline{\mathbf{z}} = \underline{\mathbf{U}}^{\text{H}}\mathbf{y}$, we have

$$T\,(\mathbf{r}) = 2\underline{\mathbf{z}}^{\text{H}}\text{diag}\,(\underline{\mathbf{v}})\,\underline{\mathbf{z}}. \tag{49}$$

It can be proved that $\text{E}\,(\underline{\mathbf{z}}) = 0$ and $\text{E}\,(\underline{\mathbf{z}}\underline{\mathbf{z}}^{\text{H}}) = \mathbf{I}$. Therefore, the test statistic in (49) follows weighted exponential distribution with the weighting vector $\underline{\mathbf{v}}$. Consequently, the detection probability of the SWD algorithm can be written as

$$p_{\text{d}} = Q\,(g, E_{\underline{\mathbf{v}}}). \tag{50}$$

The detection probability (50) applies for TFCMs with an arbitrary permissible structure.

If the target returns are statistically independent as presumed, then we have $\mathbf{Q}_{\text{t}} = \mathbf{I}$, $\mathbf{C}_{\text{t}} = \mathbf{\Lambda}_{\text{t}} = \text{diag}\,(\mathbf{E}^2)$, and

$$\underline{\mathbf{v}} = \hat{\mathbf{E}}^2\,(\mathbf{E}^2 + 1)\,/\,(\hat{\mathbf{E}}^2 + 1). \tag{51}$$

In this case, the detection probability of the SWD can be written as

$$p_d = Q \left(g, E_{\hat{\mathbf{E}}^2(\mathbf{E}^2+1)/(\hat{\mathbf{E}}^2+1)} \right). \qquad (52)$$

In addition, if the channel SNRs can be accurately estimated such that $\hat{\mathbf{E}} = \mathbf{E}$, the SWD reaches the maximum probability of detection, i.e.,

$$p_d = Q \left(g, E_{\mathbf{E}^2} \right). \qquad (53)$$

4) *Discussion*: From (31), the GGSD is composed of a whitening filter bank, whose weighting matrix is $\hat{\mathbf{Q}}_{N_r}^H \, \mathrm{diag} \, (\mathbf{p}^*)$, followed by an SWD with weighting vector $\hat{\mathbf{w}}_{N_r}$. If the envelopes of target returns are statistically independent, $\mathbf{\Theta}_t$ will be an identity matrix and then the whitening process in the GGSD can be omitted without detection performance loss. In this case, the GGSD becomes the SWD.

The SWD is optimal under two conditions. First, both the target returns and the background interferences are statistically independent; second, the SNRs of received signals are accurately known. In order to use noncoherent SWD without detection performance loss, working parameters of diversity radar are often designed to obtain statistically independent target fluctuations. For that purpose, spatial diversity radar should separate distributed radar sites sufficiently far, and frequency diversity radar should separate working frequencies sufficiently far.

In scenarios where channel SNRs are approximately the same, e.g., frequency diversity radar whose diversity channels often have identical SNRs, the SWD can be further simplified.

E. IAD

1) *Test Statistic*: In situation II, envelopes of target returns are statistically independent and diversity channels have the same SNR, i.e., $\hat{\mathbf{\Theta}}_t = \mathbf{I}$ and $\hat{E}_1 = \cdots = \hat{E}_L \equiv \hat{E}$. In this case, the detection algorithm (44) can be simplified to

$$T(\mathbf{r}) = 2\mathbf{r}^H \mathbf{r} \qquad (54)$$

which is well known as the test statistic of the IAD.

The IAD is a classical radar detection algorithm [13], which has been widely considered in researches on frequency diversity radar [15, 16] and spatial diversity radar [2, 9]. Different from the GGSD and the SWD, the IAD does not need to estimate any parameter of statistical distribution of received signals, which can greatly facilitate engineering application.

2) *False Alarm Rate*: Under the null hypothesis, from (20), $T(\mathbf{r})$ follows a Chi-square distribution with $2L$ degrees of freedom, denoted by χ_{2L}^2. Consequently, the false alarm rate can be obtained by [13]

$$p_f = Q \left(g, \chi_{2L}^2 \right). \qquad (55)$$

3) *Probability of Detection*: Under the H_1 hypothesis, we still apply the transform in (36) to the test statistic in (54) and then obtain

$$T(\mathbf{r}) = 2\mathbf{y}^H (\mathbf{\Lambda}_t + \mathbf{I}) \mathbf{y}. \qquad (56)$$

From (37), $T(\mathbf{r})$ follows a weighted exponential distribution with weighting vector $\mathbf{h}_t + 1$. Therefore, the detection probability of the IAD can be written as

$$p_d = Q \left(g, E_{\mathbf{h}_t+\mathbf{1}} \right). \qquad (57)$$

The detection probability (57) applies for any TFCM structure. Specially, if $\mathbf{\Theta}_t = \mathbf{I}$ and $\mathbf{C}_s = E\mathbf{I}$, the weighted exponential distribution becomes the Chi-square distribution with $2L$ degrees of freedom and mean $2L(E+1)$. In this case, the IAD can reach the best detection probability, given by

$$p_d = Q \left(g, (E+1) \chi_{2L}^2 \right) = Q \left(g/(E+1), \chi_{2L}^2 \right). \qquad (58)$$

4) *Discussion*: From (45), if the estimates of channel SNRs are identical or all far greater than one, the SWD would degenerate into the IAD. In other words, the IAD is approximately optimal in these situations. The performance of the IAD would degrade greatly only if channel SNRs are both low and different. In this case however, a low detection probability may not form a continuous track of a target and thus makes little sense in practice. Therefore, the IAD still draws wide attention in research on distributed MIMO radar and frequency diversity radar.

F. CAD

1) *Test Statistic*: In situation I, $\mathbf{\Theta}_t$ becomes a matrix of ones and $\Delta\mathbf{C} = EL \cdot \mathbf{p}\mathbf{p}^H / (1 + EL)$. In this case, we can obtain the test statistic of the coherent accumulating detector (CAD) from (18) as

$$T(\mathbf{r}) = 2 \left| \mathbf{p}^H \mathbf{r} \right|^2. \qquad (59)$$

2) *False Alarm Rate*: As a weighted sum of zero-mean complex Gaussian distributed variables, $\mathbf{p}^H \mathbf{r}$ follows zero-mean complex Gaussian distribution as well. Consequently, the test statistic (59) follows the Chi-square distribution with two degrees of freedom, namely the exponential distribution. It can be proved that

$$E[T(\mathbf{r})] = E \left(2 \left| \mathbf{p}^H \mathbf{r} \right|^2 \right) = 2L.$$

Therefore, the false alarm rate can be written as

$$p_f = Q \left(g, L\chi_2^2 \right) = \exp(-g/2L). \qquad (60)$$

3) *Detection Probability*: Under the H_1 hypothesis, $\mathbf{p}^H \mathbf{r}$ is still zero-mean complex Gaussian distributed and then $T(\mathbf{r})$ follows the exponential distribution. From (21), we have

$$E(T(\mathbf{r})|H_1) = 2E \left(\mathbf{p}^H \mathbf{r}\mathbf{r}^H \mathbf{p} \, | H_1 \right) = 2\mathbf{p}^H (\mathbf{C}_s + \mathbf{I}) \mathbf{p}$$
$$= 2\mathbf{1}^H (\mathbf{C}_t + \mathbf{I}) \mathbf{1} = 2F_c + 2L \qquad (61)$$

where $F_c = \sum_{i=1}^{L} \sum_{j=1}^{L} (\mathbf{C}_t)_{ij}$. Therefore, the probability of detection can be obtained by

$$p_d = \exp\left(-g/\left(2F_c + 2L\right)\right) = p_f^{L/(F_c+L)}. \quad (62)$$

From (62), as $0 < p_f < 1$, p_d is an increasing function of F_c.

In situation I, $F_c = EL^2$ and then $p_d = p_f^{1/(EL+1)}$. In situation III, $F_c = E \sum_{i=1}^{L} \sum_{j=1}^{L} \rho_{ij}$ and thus the detection probability of the CAD increases monotonically with each element of $\mathbf{\Theta}_t$. In other words, any decorrelation of target fluctuations would degrade the detection performance of the CAD.

In situation IV, $\mathbf{\Theta}_t$ is a matrix of ones and then $\mathbf{C}_t = \mathbf{E}\mathbf{E}^T$. Given a TSNR of diversity channels, such as $\sum_{i=1}^{L} E_i = EL$, we have

$$F_c = \sum_{i=1}^{L} \sum_{j=1}^{L} \sqrt{E_i}\sqrt{E_j} = \left(\sum_{j=1}^{L} \sqrt{E_i}\right)^2 \leq L \sum_{i=1}^{L} E_i = EL^2 \quad (63)$$

where the equation holds if and only if $E_1 = E_2 = \cdots = E_L$. Therefore, given the TSNR of diversity channels for situation IV, channel SNR difference would always degrade the detection performance of the CAD. The CAD is seldom used in diversity radar that tends to receive mutually decorrelated target returns. However, a coherent accumulation procedure may be used in each radar receiver to improve channel SNR and suppress interferences, such as jamming and clutter returns [35, 36].

G. Detection Algorithm for Situation IV

1) *Test Statistic*: In situation IV, target fluctuations are completely correlated, while channel SNRs are different. In this case, $\mathbf{\Theta}_t$ becomes a matrix of ones and $\mathbf{C}_t = \mathbf{E}\mathbf{E}^H$. The test statistic (18) becomes

$$T(\mathbf{r}) = 2\left|\mathbf{p}^H \text{diag}(\mathbf{E})\,\mathbf{r}\right|^2. \quad (64)$$

Based on channel SNR estimates $\hat{\mathbf{E}}$, the test statistic turns out to be

$$T(\mathbf{r}) = 2\left|\mathbf{p}^H \text{diag}\left(\hat{\mathbf{E}}\right)\mathbf{r}\right|^2. \quad (65)$$

This detection algorithm is optimal in the situations where target fluctuations are completely correlated but channel SNRs are different. It should be noted that this situation is rarely present in a practice radar and thus rarely considered before.

2) *False Alarm Rate*: As a weighted sum of zero-mean complex Gaussian distributed variables, $\mathbf{p}^H \text{diag}\left(\hat{\mathbf{E}}\right)\mathbf{r}$ follows zero-mean complex Gaussian distribution and then the test statistic (65) follows the exponential distribution. Under the null hypothesis, we have

$$\mathrm{E}\left(\left|\mathbf{p}^H \text{diag}\left(\hat{\mathbf{E}}\right)\mathbf{r}\right|^2 |H_0\right)$$
$$= \mathbf{p}^H \text{diag}\left(\hat{\mathbf{E}}\right)\mathrm{E}\left(\mathbf{r}\mathbf{r}^H|H_0\right)\text{diag}\left(\hat{\mathbf{E}}\right)\mathbf{p} = \hat{\mathbf{E}}^H\hat{\mathbf{E}}. \quad (66)$$

Therefore, the false alarm rate can be expressed by

$$p_f = \exp\left(-g/\hat{\mathbf{E}}^H\hat{\mathbf{E}}\right). \quad (67)$$

3) *Probability of Detection*: Under the H_1 hypothesis, the expectation of the test statistic becomes

$$\mathrm{E}\left(\left|\mathbf{p}^H \text{diag}\left(\hat{\mathbf{E}}\right)\mathbf{r}\right|^2 |H_1\right)$$
$$= \mathbf{p}^H \text{diag}\left(\hat{\mathbf{E}}\right)\mathrm{E}\left(\mathbf{r}\mathbf{r}^H|H_1\right)\text{diag}\left(\hat{\mathbf{E}}\right)\mathbf{p} = \hat{\mathbf{E}}^H(\mathbf{C}_t + \mathbf{I})\hat{\mathbf{E}}. \quad (68)$$

Therefore, the probability of detection can be written as

$$p_d = p_f^{\hat{\mathbf{E}}^H\hat{\mathbf{E}}/\left[\hat{\mathbf{E}}^H(\mathbf{I}+\mathbf{C}_t)\hat{\mathbf{E}}\right]}. \quad (69)$$

When $\hat{\mathbf{E}}$ in (69) becomes $\alpha\hat{\mathbf{E}}$, $\alpha \neq 0$, the detection probability remains the same. It means that the detection probability depends only on the SNR ratio of diversity channels but not on the TSNR. If $\mathbf{C}_t = \mathbf{E}\mathbf{E}^H$, then

$$p_d = p_f^{\hat{\mathbf{E}}^H\hat{\mathbf{E}}/\left[\hat{\mathbf{E}}^H\hat{\mathbf{E}}+(\hat{\mathbf{E}}^H\mathbf{E})^2\right]}. \quad (70)$$

According to Cauchy's inequity, we have $\left(\hat{\mathbf{E}}^H\mathbf{E}\right)^2 \leq \left(\hat{\mathbf{E}}^H\hat{\mathbf{E}}\right)\left(\mathbf{E}^H\mathbf{E}\right)$, where the equation holds if and only if $\hat{\mathbf{E}} = \alpha\mathbf{E}$ where α is an arbitrary constant. Therefore, we can obtain

$$p_d \leq p_f^{\hat{\mathbf{E}}^H\hat{\mathbf{E}}/\left[\hat{\mathbf{E}}^H\hat{\mathbf{E}}+(\hat{\mathbf{E}}^H\hat{\mathbf{E}})(\mathbf{E}^H\mathbf{E})\right]} = p_f^{1/[1+(\mathbf{E}^H\mathbf{E})]} \quad (71)$$

which is also the highest detection probability of the test statistic (70).

So far, five detection algorithms have been discussed for five typical situations presented in Table I. The detection algorithm for situation III is very similar to the GGSD and thus is not discussed here. Though different in signal processing method and detection performance, these target detection algorithms can be incorporated into the same signal processing framework, i.e., a whitening process to transform input signals into statistically independent channels and a following SWD to apply different weights to signals in these channels. The detection algorithms differ in the whitening weights and the weights applied to the independent channels, which are summarized in Table II.

In practice, both the whitening process and the weighting process may induce a detection performance loss. Therefore, correlation of target fluctuations and channel SNRs should be accurately estimated in order to achieve the optimal detection performance. An interesting problem is how much detection performance loss the concerned detection algorithms would have when the

Detection Algorithms	Whitening Weight	SNR Weight
GGSD	$\hat{\mathbf{Q}}_t$	$\hat{\mathbf{w}}_t$
SWD	$\mathbf{I}$	$\hat{\mathbf{E}}^2 / \left(\hat{\mathbf{E}}^2 + 1 \right)$
IAD	$\mathbf{I}$	1
CAD	$\mathbf{p}$	$\mathbf{e}_1$
That for situation IV	$\mathrm{diag}\left(\hat{\mathbf{E}} \right) \mathbf{p}$	$\mathbf{e}_1$

Note: $\mathbf{e}_1$ is the first column of the identity matrix of the proper size.

estimation is inaccurate. If the estimation is accurate, another interesting problem is what the optimal detection performance will be for different degrees of target correlation and different channel SNR ratios. In the following section, we present numerical results for typical situations to study these problems.

IV. DETECTION PERFORMANCE OF DIVERSITY RADAR

There are various types of diversity radar, such as spatial diversity radar, frequency diversity radar, and their combination SFDR. However, from preceding analysis, for spatial diversity channels, frequency diversity channels, and spatial-frequency jointly diversity channels, the correlation coefficient of target returns depends only on target size and the EFI. Therefore, in this section, we do not specify exact type of diversity radar pairs for simplicity. We instead assign the EFIs of the diversity channel, pairs or directly, the correlation coefficient of target returns. The results can be straightforwardly applied to spatial diversity radar, frequency diversity radar, and their combination.

On the contrary of diversity radar, a nondiversity radar system can observe only one aspect of a radar target per observation, even if it may have multiple receiving channels. A radar system with only one channel or multiple channels receiving completely correlated target returns would subsequently be deemed as nondiversity radar.

The detection performance of a diversity radar system depends on the degree of diversity of its received signals. Given a bunch of received signals, the degree of diversity relies on three factors, i.e., the number of signals, mutual correlation of target components, and the SNRs of the

signals. For instance, completely correlated target returns evidently have less degree of diversity than independent ones. If the power of the target components concentrates only in a diversity channel, the degree of diversity is minimal. If the power of target components is uniformly distributed into all diversity channels, the degree of diversity would increase.

The impact of the number of signals on the detection performance of diversity radar has been studied in [2, 13]. In this work, we focus on the left two factors, i.e., correlation of target returns and SNR of signals. The range phase terms have a great impact on the detection performance of coherent detection algorithms as well, such as the GGSD and the CAD, but as we do in theoretical analysis, they are assumed to be exactly known a priori. We still assume that background noises in diversity channels are statistically independent of each other. The false alarm rate, decision gate, and detection probability are all connected with the weighted exponential distribution, whose cdf is directly calculated by using the method proposed in [34]. The false alarm rate would be set by 10^{-4} if not specified.

A. Influence of Correlation of Target Returns

Most of detection algorithms for diversity radar were designed and evaluated under the assumption that target components in diversity channels are statistically independent [2]. In order to study the detection performance of the detection algorithms for correlated target returns, we consider a diversity radar system with two diversity channels of the same SNR. If the target components are correlated with correlation coefficients of 0, 0.6, 0.9, and 1, Figs. 2(a)–2(d) show the probabilities of detection versus channel TSNR, respectively.

Assume that the GGSD has the exact knowledge of correlation coefficients of target returns. Therefore, the GGSD provides the highest detection probability. Compared with the GGSD, the CAD can reach the maximal detection probability when $\rho = 1$ from Fig. 2(d), while the IAD algorithm can reach the maximal detection probability when $\rho = 0$ from Fig. 2(a). For partially correlated target returns, both the CAD and the IAD suffer from detection performance loss. Specifically, for partially correlated target returns, the IAD performs better than the CAD at high TSNRs and worse at low TSNRs.
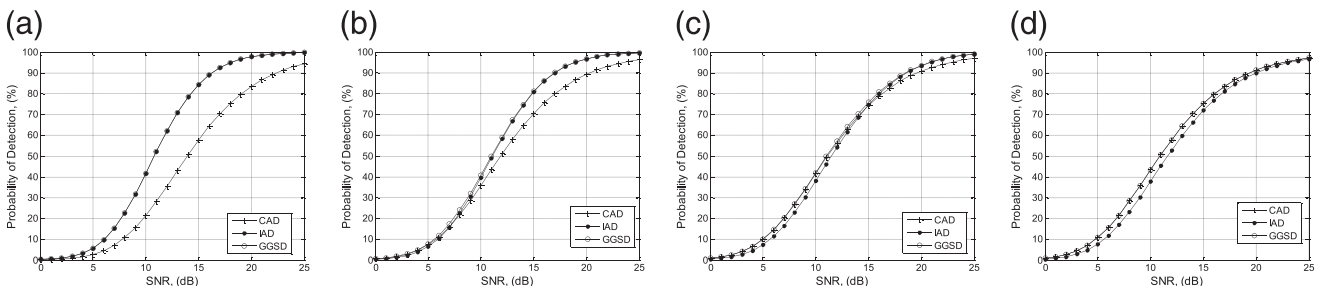
(a) (b) (c) (d)

Fig. 2. Detection probability versus TSNR at target correlation coefficients of (a) 0, (b) 0.6, (c) 0.9, and (d) 1.
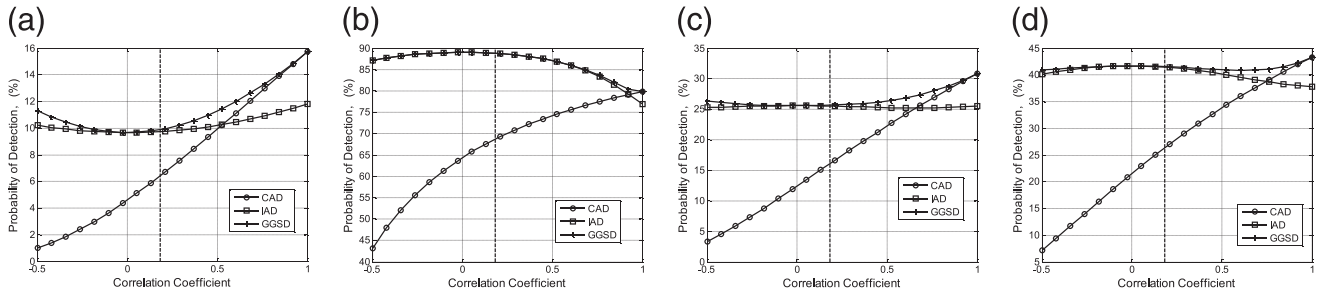
Fig. 3. Detection probabilities versus correlation coefficient of target fluctuations for two diversity channels with TSNRs of (a) 6 dB, (b) 16 dB, (c) 8.35 dB, and (d) 10 dB. Dashed line denotes independence criterion with $\varepsilon = 1$.

Given TSNR of two diversity channels, the degree of correlation of target returns has a great impact on the detection performance of detection algorithms. If the TSNRs are 6 dB, 16 dB, 8.35 dB, and 10dB, the detection probabilities versus the correlation coefficient of target fluctuations are shown in Figs. 3(a)–3(d), respectively.

From Figs. 3(a)–3(d), the detection probability of the CAD is always an increasing function of the correlation coefficient, in agreement with previous theoretical analysis, whereas the monotonicity of the detection probabilities of both the IAD and the GGSD depends on the TSNR available. If the TSNR is high, such as the TSNR = 16 dB case, they decrease with the absolute value of the correlation coefficient; if it is low, say 6 dB, they may increase with the correlation coefficient, although the detection performance loss of the IAD increases in this case.

For the IAD, we find that at about 8.35 dB, the target detection probability versus the target correlation coefficient is approximately a constant 25.4%, as shown in Fig. 3(c). It should be noted that the detection probability of the IAD versus the correlation coefficient at this TSNR still has slight fluctuation. No TSNR is found so far that can make the optimal detection probability versus the correlation coefficient approximately a constant. As the correlation coefficient increases, the optimal detection probability may first decrease and then increase, as shown in Fig. 3(d). Fig. 3(d) also shows that the GGSD and the IAD may reach their best detection performances at different correlation levels of target returns. In Figs. 3(a)–3(b), the IAD and the GGSD have the same monotonicity, whereas in Fig. 3(d), they do not keep the same monotonicity.

More experiments indicate that the optimal detection probability, given by the GGSD, may reach a minima for any correlation coefficient, but the highest optimal detection probability would be present at either $\rho = 0$ or $\rho = \pm 1$ but would not be present over $0 < |\rho| < 1$. Therefore, it means that at least for the case of two diversity channels, one may expect either completely correlated target returns or independent ones for better optimal detection performance, if only we can control the correlation of target returns.

In Figs. 3(a)–3(d), the dashed lines are drawn according to the independence criterion with strictness factor $\varepsilon = 1$ [see formula (5)]. The correlation coefficient with respect to the independence criterion is 0.1812. From Figs. 3(a)–3(d), at the point with respect to this strictness factor, the IAD and the GGSD have higher detection probabilities than the CAD for the TSNRs. Therefore, if one just selects a detection algorithm from the CAD and the IAD, the strictness factor may be relaxed to $\varepsilon = 0.5$, for which $\rho = 0.7217$ and near this value the two detectors have closer detection probabilities.

Correlation of target returns depends on two factors, i.e., target size and channel EFI. Each point in space corresponds to an EFI and its spatial distribution can be determined for radar with specific settings [17]. Although we cannot control which targets would be present in space and their sizes, we can control the EFIs between diversity channels to some extent. In order to study the impact of the EFI on the detection performance of diversity radar, we consider a diversity radar with two diversity channels. Assume that the target in presence is 10 m in length. Figs. 4(a) and 4(b) show the detection probabilities of the CAD, the IAD, and the GGSD versus the EFI for TSNRs of 6 dB and 16 dB, respectively.

It can be seen from Fig. 4 that the detection probabilities of these algorithms often fluctuate as the EFI increases. That is because the correlation coefficient is not a monotonic function of the EFI [17]. Compared with the optimal detection algorithm provided by GGSD with exact knowledge of target size, the CAD would reach the optimal detection performance for $f_e = 0$ and the IAD has nearly optimal detection performance for high EFIs.

It can be expected that the mismatch between presumed target size and real target size may induce detection performance loss. This fact can be found in Fig. 4. The performance loss due to target size mismatch is given by the GGSD using $d = 20$ m. It can be found that the GGSD with a mismatched target size can still perform close to the optimal performance (provided by the GGSD using $d = 10$ m) when $f_e = 0$ (the GGSD degenerates into the CAD) and the EFI is high (the GGSD degenerates into the IAD). In comparison with the optimal detection performance, the GGSD using $d = 20$ m only suffers a slight performance loss when target returns are partially correlated. Therefore, although mismatch in target size is inevitable in practice, the GGSD with slight target size mismatch may provide an acceptable detection probability
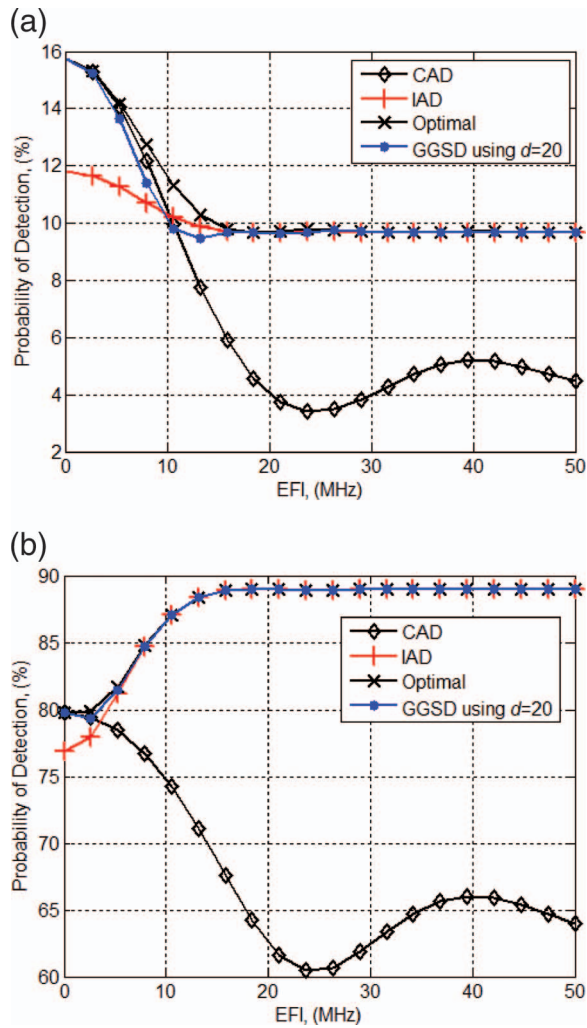
(a)

(b)

Fig. 4. Detection probability versus EFI of two diversity channels at TSNRs of (a) 6 dB and (b) 16 dB.

Fig. 5. ROC curves of IAD and GGSD for partially correlated target returns at TSNRs of 7 dB and 11 dB.

over the whole EFI range. Detectors not concerning target correlation and channel SNRs (e.g., the CAD and the IAD) often suffer from a significant loss at either a zero EFI or a great EFI.

The evidence that inaccurate assumption on target size would degrade the detection performance of the GGSD can also be found in other figures by examining detection probabilities of the CAD and the IAD. That is because if partially correlated target returns are received, the CAD can be considered as the GGSD using an underestimated target size, and the IAD as the GGSD using an overestimated target size.

Radar detection is often carried out at a prescribed CFAR and the false alarm rate has a great impact on the detection performance. For two partially correlated target returns with correlation coefficients of 0.6 and 0.9, the receiver operating characteristic (ROC) curves of the IAD and the GGSD are all given in Fig. 5 when TSNRs are 7 dB and 11 dB. Since the CAD is not so widely used in diversity radar, its ROC curve is not given here to avoid the curves being too crowded.

From Fig. 5, for the GGSD and the IAD fed by two signals with certain TSNR, whether a lower degree of
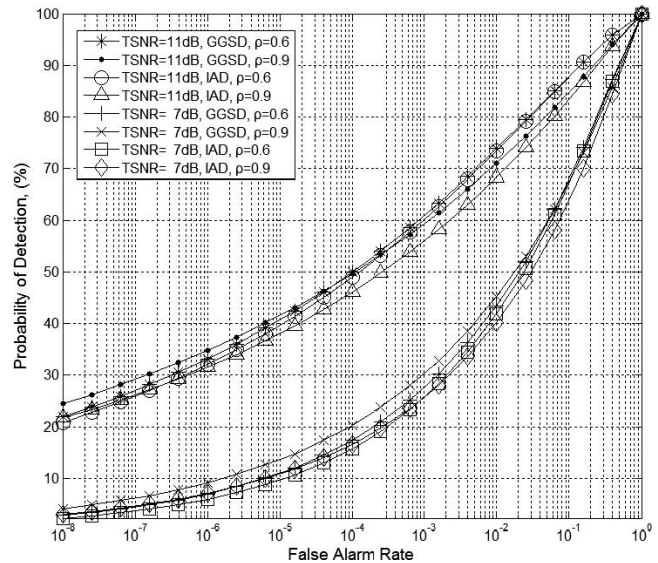
correlation of target returns can give a higher detection performance depends a great deal on the false alarm rate prescribed. At a high false alarm rate, a lower degree of correlation of target returns will give a better detection performance, and at a higher false alarm rate, a higher degree of correlation of target returns will give a better detection performance. Fig. 5 demonstrates that if the TSNR is 11 dB, $\rho = 0.6$ and $\rho = 0.9$ would give the same optimal detection probability at the false alarm rate of about 10^{-4}. For the IAD, the transition point of the false alarm rate is much lower. Moreover, the transition point varies with the TSNR available. In practice, commonly used false alarm rates are often in an interval say $[10^{-6}, 10^{-3}]$ over which certain correlation of target returns may always precede another in detection performance.

To conclude, first, the correlation of target returns has a great impact on the target detection performance of diversity radar. Second, when target returns are partially correlated, the GGSD with exact target size information can improve the detection performance in contrast with the IAD and the CAD. Third, whether a lower degree of correlation of target returns benefits the optimal detection performance depends on the TSNR available and the prescribed false alarm rate.

B. Influence of Channel SNR Distribution

Multisite radar systems tend to receive target returns of different SNRs for many reasons. Optimal likelihood ratio test (LRT) and generalized LRT (GLRT) algorithms with known different SNRs for distributed radars have been synthesized in [13] for signals with mutually correlated and uncorrelated fluctuations. Many detection algorithms are based on the assumption that diversity channels have the same SNR [2, 9, 13]. In what follows, using concerned detection algorithms, we would study the detection performance of diversity radar when channel SNRs are different.
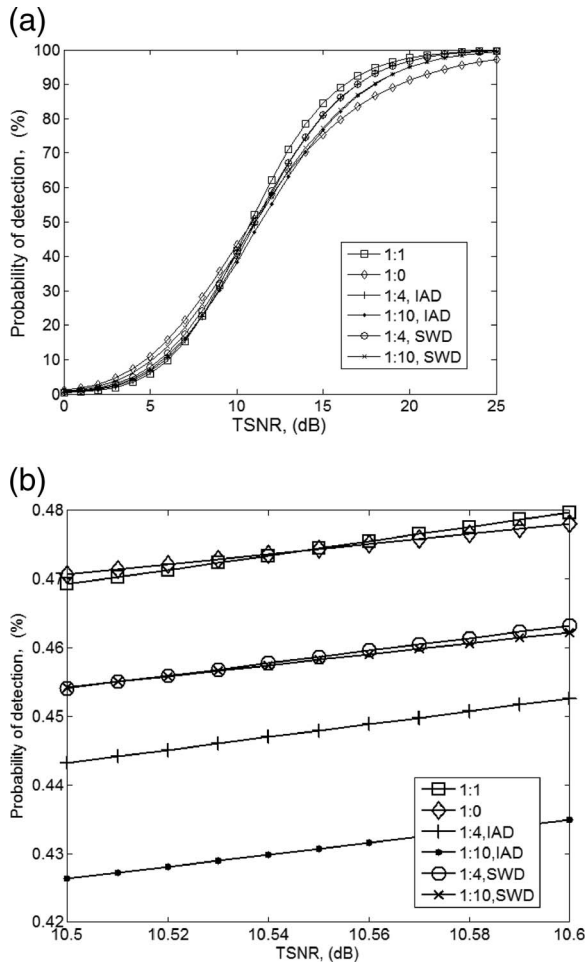
(a)

(b)

Fig. 6. Detection probabilities of diversity radar versus TSNR. (a) Different channel SNRs. (b) Closer view at TSNRs around 10.54 dB.

We still consider a diversity radar system with two diversity channels, in which the target returns are perfectly independent but have different SNRs. In this case, the SWD using exact knowledge of channel SNRs would achieve the optimal detection performance. When channel SNR ratios of the two channels are 1:1, 1:0, 1:4, and 1:10, the detection probabilities of the IAD and the SWD are shown in Fig. 6(a). Fig. 6(b) is given to make a closer view around TSNR = 10.5 dB. The SNR ratio 1:0 refers to the case in which all target power falls in one channel and the detection probability is evaluated only for the channel with nonzero power of target returns.

From Fig. 6(a), with exact knowledge of channel SNRs, the SWD provides the optimal detection performance and thus has a better detection performance than that of the IAD. In agreement with the theoretical analysis in Section III-D.1, the detection performance of the IAD approximates to the SWD when channel SNRs are all high. The detection performance loss of the IAD is present mainly in situations where channel SNRs are both low and different.

From Fig. 6(a), returns with equal SNRs do not always have a better detection performance. It depends on the TSNR available. Fig. 6 demonstrates that at high TSNRs,
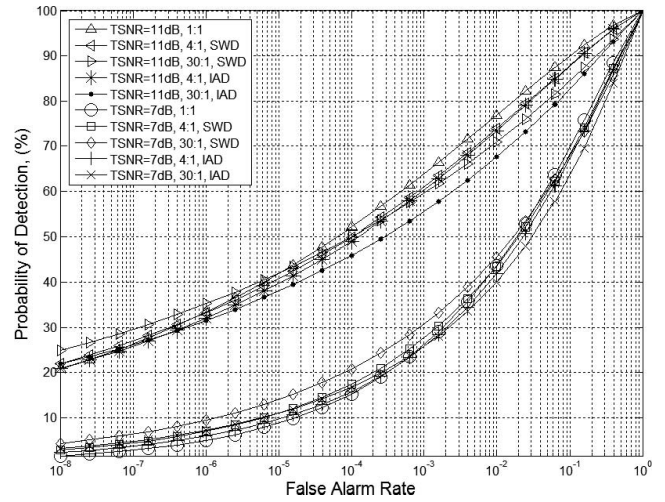

Fig. 7. ROC curves of IAD and SWD for different channel SNRs for TSNRs of 7 dB and 11 dB.

the optimal detection performance would reach a peak when target power is uniformly distributed into two diversity channels, while at low TSNRs, the peak is reached when target power concentrates on one channel. For the case at hand, unequal channel SNRs have no opportunity to make the optimal detection probability reach the peak at any TSNR. This fact can be found from Fig. 6(b). Therefore, SNR unbalance is harmful to the optimal detection performance of diversity radar.

False alarm rate also has a great impact on the detection performance. In order to study its impact, consider two signals with TSNRs of 7 dB and 11 dB. The ROC curves of the SWD and the IAD are shown in Fig. 7 when SNR ratios are 1:1, 4:1, and 30:1.

From Fig. 7, the detection probability of the SWD is higher than that of the IAD and the difference in detection probability increases with the channel SNR. Given a TSNR, at high false alarm rates, uniform channel SNRs would give rise to the highest optimal detection probability, while at low false alarm rates, more unbalanced channel SNRs would produce a better optimal detection performance.

For the SWD, inaccurate estimation of channel SNRs would result in a detection performance loss, but we do not give a separate simulation result here, because the IAD can be considered as the SWD erroneously presuming that channel SNRs are identical.

To conclude, the SWD can improve the detection performance of diversity radar if channel SNRs can be estimated accurately. Even for different channel SNRs, the IAD can approach the optimal detection performance when both channel TSNR and false alarm rate are high. Given TSNR and false alarm rate, the optimal detection probability depends on the ratio of channel SNRs. For high TSNRs and high false alarm rates, signals with uniform SNRs would give a better detection performance, whereas for low TSNRs and low false alarm rates, channel SNRs that are more different would give a better detection performance.

C. Relationship between Target Correlation and SNR Distribution

Target correlation and balanced channel SNR are two different kinds of radar diversity. But from Figs. 5 and 7, the ROC curves have a similar appearance. In fact, there is a certain inherent relationship between the two kinds of radar diversity. For correlated target returns, from (30), the optimal detection algorithm given by (18) can be written as

$$T(\mathbf{r}) = 2\mathbf{r}^H \text{diag}(\mathbf{p}) \mathbf{Q}_t \frac{\mathbf{\Lambda}_t}{\mathbf{\Lambda}_t + \mathbf{I}} \mathbf{Q}_t^H \text{diag}(\mathbf{p}^*) \mathbf{r}. \quad (72)$$

From (72), by using the whitening matrix $\mathbf{Q}_t^H \text{diag}(\mathbf{p}^*)$, the optimal detection algorithm would first transform original received signals into independent ones wherein both noise components and target components are statistically independent. An SWD is followed to weight the output signals according to the SNRs of the independent channels.

In the ideal situation, the target covariance matrix is exactly known to the GGSD and then the GGSD can transform correlated target returns into statistically independent components. If target returns are partially correlated, after the transformation, target returns originally with the same SNR may give rise to independent components with different SNRs. For instance, if two target returns have correlation coefficient 0.6 and their SNRs are identical, the SNR of the statistically independent components is 4:1. It can be easily proved that for two diversity channels with identical channel SNRs, a higher correlation coefficient of target returns would result in independent components that are more different in SNR. In other words, it is the SNR distribution of the independent components that determines the optimal detection performance of diversity radar. The correlation of target returns changes the optimal detection performance through changing SNRs of the independent components.

From (72), four parameters corresponding to statistical distribution of received signals should be accurately estimated in order to reach the optimal detection performance, i.e., channel range phase terms, interference covariance matrix, correlation coefficients of target returns, and SNRs of diversity channels. By assumption, the range phase terms are known a priori and the interference covariance matrix is an identity matrix. We just focus on the correlation coefficients and the channel SNRs. Inaccurate estimation of any parameter may induce a detection performance loss.

D. Scenario of more Diversity Channels

So far we mainly study the case with two diversity channels for simplicity. In this case, the difference of detection performance between different detection algorithms is insignificant and the advantage of diversity radar in detection performance is not so obvious. Now consider a diversity radar system with six active diversity channels and the SNR ratio is 10:10:5:5:1:1. Meanwhile,
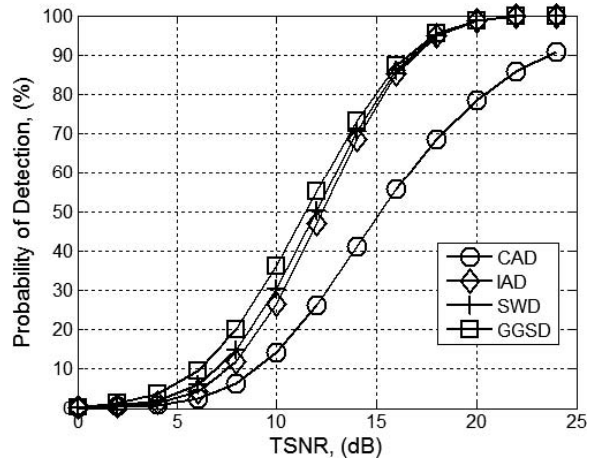

Fig. 8. Detection probabilities of four detection algorithms for six diversity channels with different channel SNRs and partially correlated target returns.

the correlation coefficient matrix of target returns is given by

$$\mathbf{\Theta}_t = \begin{bmatrix} 1 & 0.9 & 0.8 & 0 & 0 & 0 \\ 0.9 & 1 & 0.7 & 0 & 0 & 0 \\ 0.8 & 0.7 & 1 & 0 & 0 & 0 \\ 0 & 0 & 0 & 1 & 0 & 0 \\ 0 & 0 & 0 & 0 & 1 & 0 \\ 0 & 0 & 0 & 0 & 0 & 1 \end{bmatrix} \quad (73)$$

The GGSD still has the exact knowledge of all distribution parameters and hence gives the maximal detection probability. The SWD has the SNR knowledge but it by mistake assumes that target returns are statistically independent. The detection probabilities of the concerned detection algorithms are all shown in Fig. 8.

From Fig. 8, with six diversity channels available, the improvement of the GGSD in detection probability is more significant. The SWD suffers from a little detection performance loss, because there are three target returns partially correlated. Without considering both correlation of target returns and SNR distribution of diversity channels, the IAD suffers from a greater detection performance loss. The CAD performs the worst, because most signals are statistically independent from (73).

V. CONCLUSION AND DISCUSSION

We introduced the method to estimate the correlation coefficient of target returns received by a complicated SFDR in which target returns may be partially correlated and different in SNR. It was pointed out that in diversity radars, especially the SFDR, target returns in diversity channels tend to be partially correlated and to have different SNRs. Therefore, according to channel SNR distribution and target correlation, six scenarios are considered, for which several detection algorithms were developed according to the Neyman-Pearson criterion, such as the GGSD, the SWD, and the well-known IAD. The detection performance of concerned detection

algorithms is analyzed in theory and via numerical results in scenarios when target returns are partially correlated and have different SNRs. Meanwhile, the conditions on which those detection algorithms can reach the peak detection performance are studied. The GGSD can achieve optimal detection performance of diversity radar even for partially correlated target returns if target correlation and channel SNRs can be accurately estimated. If target returns are statistically independent but different in SNR, the SWD can improve the detection performance in comparison with the IAD. If target returns are statistically independent, the IAD can still give acceptable detection performance when channel SNRs are either identical or all very high.

We also studied the optimal detection performance of diversity radar by using the GGSD when target returns are partially correlated and channel SNRs are different. It was found that whether a diversity radar has a better detection performance than a nondiversity one depends on the TSNR available and the false alarm rate. If the TSNR and false alarm rate are high, diversity radar would perform better and vise versa. A low TSNR and low false alarm rate may not produce a detection probability sufficient to form a continuous target track and then in practice, we are often interested in a high detection probability, for which diversity radar takes an advantage in detection performance. Therefore, diversity radar takes an advantage over nondiversity radar in detection performance.

Given TSNR and false alarm rate, the optimal detection performance of diversity radar depends on the degree of diversity of received signals. Two kinds of diversity were considered, i.e., correlation of target returns and channel SNR distribution. The relationship between two kinds of diversity was studied and it was found that the correlation of target returns affects optimal detection performance of diversity radar by affecting SNRs of independent components of received signals. The optimal detection performance is actually determined by SNRs of the independent components. Whether a channel SNR can produce a better detection performance than another channel SNR depends on the TSNR available and the false alarm rate.

In engineering practice, the detection algorithm to choose depends not only on the detection performance of the detection algorithms, but also on the cost of implementing them. One needs to make a tradeoff between detection performance and system complexity. Although the GGSD can reach the maximal detection probability, it needs to estimate many statistical distribution parameters of received signals and to use a complicated whitening-weighting scheme. The SWD does not need the whitening processing but still needs to estimate channel SNRs. In some situations, the IAD can be applied as if the detection performance loss is acceptable because it requires the simplest signal processing scheme.

In practice, for a better detection performance and a simple system structure, target returns that are statistically independent and have the same SNR are still desirable. In fact, one can partially control statistical correlation of target returns by properly selecting parameters of a radar system according to an independence criterion. In order to make the channel SNRs close, one can properly deploy distributed radar sites such that they have close distances from the surveillance space of interest.

In order to make a signal fusion based detection, a signal fusion center of a distributed MIMO radar should also make spatial alignment and time alignment to received signals with respect to the same spatial resolution cell. Meanwhile, we can also make a coherent accumulation in each diversity channel separately, which can improve channel SNR and enable clutter rejection. Signal fusion based detection places a high demand on the communication link between radar sites and an interesting work is how to decrease the communication burden at the cost of an acceptable detection performance loss.

REFERENCES

[1]   Fishler, E., Haimovich, A., Blum, R., Chizhik, D., Cimini, L., and Valenzuela, R.
      MIMO radar: An idea whose time has come.
      In *Proceedings of the IEEE Radar Conference*, Philadelphia, PA, 2004, pp. 71–78.

[2]   Fishler, E., Haimovich, A., Blum, R. S., Cimini, L., Chizhik, D., and Valenzuela, R.
      Spatial diversity in radars - Models and detection performance.
      IEEE Transactions on Signal Processing, **54** (2006), 823–838, 2006.

[3]   Robey, F. C., Coutts, S., Weikle, D., McHarg, J. C., and Cuomo, K.
      MIMO radar theory and experimental results.
      In *Conference Record of the Thirty-Eighth Asilomar Conference on Signals, Systems and Computers*, 2004, pp. 300–304.

[4]   Li, J., and Stoica, P.
      MIMO radar with colocated antennas.
      IEEE Signal Processing Magazine,, **24** (2007), 106–114.

[5]   Chernyak, V. S.
      On the concept on MIMO radar.
      In *IEEE Radar Conference* Washington, DC, 2010, pp. 327–332.

[6]   Chernyak, V. S.
      MIMO radars: What are they?
      In *Proceedings of European Radar Conference* Paris, 2010, pp. 137–140.

[7]   Xu, L. Z., Li, J., and Stoica, P.
      Target detection and parameter estimation for MIMO radar systems.
      IEEE Transactions on Aerospace and Electronic Systems, **44** (2008), 927–939.

[8]   Zhou, S., Liu, H., Liu, B., and Yin, K.
      Adaptive MIMO radar target parameter estimation with Kronecker-product structured interference covariance matrix.
      Signal Processing, **92** (2012), 1177–1188.

[9]   Haimovich, A. M., Blum, R. S., and Cimini, L. J.
      MIMO radar with widely separated antennas.
      IEEE Signal Processing Magazine, **25** (2008), 116–129.

[10] Li, J., Stoica, P., Xu, L. Z., and Roberts, W.
      On parameter identifiability of MIMO radar.
      IEEE Signal Processing Letters, **14** (2007), 968–971.

[11] Xu, L., Stoica, P., and Li, J.
      Parameter estimation and number detection of MIMO radar targets.

In *Conference Record of the Forty-First Asilomar Conference on Signals, Systems and Computers*, 2007 (ACSSC 07), 2007, pp. 177–181.

[12] Zhou, S. H., Liu, H. W., Liu, B. C., and Yin, K. Y.
Colocated MIMO radar beamforming with two sides adaptivity.
In *IEEE Radar Conference* 2011, vol I 2011, pp. 104–107.

[13] Chernyak, V. S.
Fundamentals of Multisite Radar Systems: Multistatic Radars and Multiradar Systems. Amsterdam: Gordon and Breach Science Publishers, 1998.

[14] Lehmann, N. H., Haimovich, A. M., Blum, R. S., and Cimini, L. A. C. L.
High resolution capabilities of MIMO radar.
In *Fortieth Asilomar Conference on Signals, Systems and Computers, 2006* (ACSSC '06), 2006, pp. 25–30.

[15] Vannicola, V.
Detection of slow fluctuating targets with frequency diversity channels.
IEEE Transactions on Aerospace and Electronic Systems, **AES-10** (1974), 43–52.

[16] Fante, R. L.
Multifrequency detection of a slowly fluctuating target.
IEEE Transactions on Aerospace and Electronic Systems, **32** (1996), 495–497.

[17] Zhou, S. H., and Liu, H. W.
Target statistical correlation characteristic for spatial-frequency jointly diversity MIMO radar.
IET Radar, Sonar & Navigation, **5** (2011), 638–649.

[18] Jung, B. W., Adve, R. S., Chun, J., and Wicks, M. C.
Detection performance using frequency diversity with distributed sensors.
IEEE Transactions on Aerospace and Electronic Systems, **47** (2011), 1800–1813.

[19] Swerling, P.
Probability of detection for fluctuating targets.
IEEE Transactions on Information Theory, **IT-6** (1960), 269–308.

[20] Sammartino, P. F., Baker, C. J., and Griffiths, H. D.
Target model effects on MIMO radar performance.
In *Proceedings of International Conference on Acoustics, Speech and Signal Processing, 2006* (ICASSP 2006), 2006, pp. V–V.

[21] Aittomaki, T., and Koivunen, V.
Performance of MIMO radar with angular diversity under Swerling scattering models.
IEEE Journal of Selected Topics in Signal Processing, **4** (Feb. 2010), 101–114.

[22] Zhou, S., Xu, X., Hu, L., and Liu, H.
Research for scattering properties of spatial and frequency diversity MIMO radar targets.
In *International Conference on Signal Processing Proceedings (ICSP)*, Beijing, China, 2008, pp. 2533–2537.

[23] Farina, A., and Russo, A.
Radar detection of correlated targets in clutter.
IEEE Transactions on Aerospace and Electronic Systems,, **AES-22** (1986), 513–532.

[24] Lehmann, N. H., Fishler, E., Haimovich, A. M., Blum, R. S., Chizhik, D. A., Cimini, L. J., and Valenzuela, R. A.
Evaluation of transmit diversity in MIMO-radar direction finding.
IEEE Transactions on Signal Processing, **55** (2007), 2215–2225.

[25] Aittomaki, T., and Koivunen, V.
Target detection and positioning in correlated scattering using widely distributed MIMO radar.
In *Proceedings of EuRAD*, Paris, 2010, pp. 403–406.

[26] Zhou, S. H., Liu, H. W., Zhao, Y. B., and Hu, L. B.
Target spatial and frequency scattering diversity property for diversity MIMO radar.
Signal Processing, **91** (2011), 269–276.

[27] Poor, H. V. *An Introduction to Signal Detection and estimation*.
New York: Springer-Verlag, 1994.

[28] Deng, H.
Polyphase code design for orthogonal netted radar systems.
IEEE Transactions on Signal Processing, **52** (2004), 3126–3135.

[29] Bo, L., and Zishu, H.
Comments on discrete frequency-coding waveform design for netted radar systems.
IEEE Signal Processing Letters, **15** (2008), 449–451.

[30] Van Trees, H. L. *Detection, Estimation, and Modulation Theory - Part III: Radar-Sonar Signal Processing and Gaussian Signals in Noise*, vol. III. New York: Wiley, 2001.

[31] Zhe, Z., and Fuhrmann, D. R.
Complex point target models for multistatic radar.
In *2008 42nd Asilomar Conference on Signals, Systems and Computers*, 2008, pp. 624–628.

[32] Siegman, A. E. *Lasers.* Mill Valley, CA: University Science Books, 1986.

[33] Bhargava, R. P., and Khatri, C. G.
The distribution of product of independent beta random variables with application to multivariate analysis.
Annals of the Institute of Statistical Mathematics, **33** (1981), 287–296.

[34] Castaño-Martínez, A., and López-Blázquez, F.
Distribution of a sum of weighted central chi-square variables.
Communications in Statistics - Theory and Methods, **34** (2005), 515 –524.

[35] Zhou, S. H., and Liu, H. W.
Signal fusion-based target detection algorithm for spatial diversity radar.
IET Radar, Sonar & Navigation, **5** (2011), 204–214.

[36] Zhou, S. H., Wang, H. X., Hu, L. B., and Liu, H. W.
Signal fusion network for spatial diversity MIMO radar.
In *IET Radar Conference*, Guilin, China, 2009.

Hongwei Liu (M'00) received the B.Eng. degree from Dalian University of Technology in electronic engineering in 1992, and the M.Eng. and Ph.D. degrees in electronic engineering from Xidian University, Xi'an, China, in 1995 and 1999, respectively.

He is currently the director of and a professor with the National Laboratory of Radar Signal Processing, Xidian University. His research interests include radar automatic target recognition, radar signal processing, and adaptive signal processing.

Shenghua Zhou received the B.Eng. and Ph.D. degrees from Xidian University, Xi'an, China, in 2005 and 2011, respectively.

He is currently an associate professor with the National Laboratory of Radar Signal Processing, Xidian University. His research interests include but are not limited to MIMO radar, multisite radar, radar target detection, statistical signal processing, and radar waveform design.

Hongtao Su received the B.Eng., M.Eng., and Ph.D. degrees in electronic engineering from Xidian University, Xi'an, China, in 1997, 2000, and 2005, respectively.

He is currently a professor with National Key Laboratory of Radar Signal Processing, Xidian University. His main research interests are in the fields of HF OTHR signal processing, adaptive array signal processing, and statistical signal processing.

Yao Yu received the B.S. degree in telecommunication engineering from Xidian University, Xian, China, in 2005, and the M.Phil. degree from City University of Hong Kong, Hong Kong, in 2007. She received her Ph.D. degree in electrical engineering from Drexel University, Philadelphia, PA, in 2010.

She is currently with Rutgers, The State University of New Jersey. Her research interests currently include wireless communication and digital signal processing.